Marine Geology 441 (2021) 106598

Contents lists available at ScienceDirect

Marine Geology

journal homepage: www.elsevier.com/locate/margo

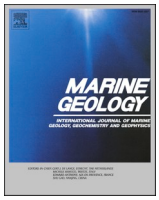

Recent morpho-sedimentary processes in Dove Basin, southern Scotia Sea, Antarctica: A basin-scale case of interaction between bottom currents and mass movements

F.J. Lobo [a,*], A. López-Quirós [a,b], F.J. Hernández-Molina [c], L.F. Pérez [d], M. García [e], D. Evangelinos [a], F. Bohoyo [f], J. Rodríguez-Fernández [a], A. Salabarnada [a], A. Maldonado [a]

[a] Instituto Andaluz de Ciencias de la Tierra, CSIC-Universidad de Granada, Avda. de las Palmeras 4, 18100 Armilla, Granada, Spain
[b] Department of Geoscience, Aarhus University, Høegh-Guldbergs Gade 2, 8000 Aarhus c, Denmark
[c] Department of Earth Sciences, Royal Holloway University of London, Egham, Surrey TW20 0EX, UK
[d] British Antarctic Survey, High Cross, Madingley Road, Cambridge CB3 0ET, UK
[e] Instituto Español de Oceanografía, Centro Oceanográfico de Cádiz, Muelle Pesquero s/n, 11006, Cádiz, Spain
[f] Instituto Geológico y Minero de España, Ríos Rosas 23, 28003, Madrid, Spain

ARTICLE INFO

Editor: Michele Rebesco

Keywords:
Scotia Sea
Dove Basin
Sub-bottom stratigraphy
Contourites
Gravity flows
Weddell Sea Deep Water
Antarctic Circumpolar Current

ABSTRACT

Multibeam bathymetric imagery and acoustic sub-bottom profiles are used to reveal distribution patterns of subsurface sedimentation in Dove Basin (Scotia Sea). The goals of the study are to determine the imprint of the inflow of deep Antarctic water masses from the Weddell Sea into the Scotia Sea, to establish the factors driving the styles of contourite deposition and to discern the relative contribution of alongslope versus downslope processes to the construction of the uppermost late Quaternary sedimentary record in the basin.

The most significant morpho-sedimentary features in Dove Basin are linked to contouritic processes and to mass movements. Plastered drifts on the flanks of the basin constitute the most common contouritic deposits. Basement-controlled drifts on top of structural elevations are common along the central ridge, the central basin plain and scattered along the basin flanks. Sheeted drifts occur on top of adjacent banks or are restricted to the deep basin. In contrast, mounded drifts are poorly represented in Dove basin. A laterally extensive contouritic channel runs along the central ridge. Contouritic channels are also identified in the upper parts of the lateral banks and slopes. Numerous slide scars along the upper parts of the slopes evolve downslope into semi-transparent lens-shaped bodies, with occasional development of across-slope channels. Semitransparent lenses occur intercalated within stratified deposits in the slopes of the basin, in the central ridge and in the deepest basin plain.

The spatial arrangement of contouritic morphologies points to the influence of the water column structure and the basin physiography. In the eastern sub-basin, two different fractions (lower and upper) of Weddell Sea Deep Water (WSDW) leave an imprint on contourite deposits owing to the sloping interface between the two fractions. Contouritic influence is more subdued in the western sub-basin, and limited to the imprint of the lower WSDW. The upper parts of the surrounding banks are under the influence of deep-reaching Circumpolar waters (i.e., Lower Circumpolar Deep Water), which develops both depositional and erosional morphologies. The cross-section V-shaped morphology of the basin and the common occurrence of structural highs drive the predominance of plastered and basement-controlled drifts in the sediment record. The frequent alternation between contourites and downslope gravity-flow deposits is likely due to different processes associated with over-steepening in the basin, such as basement-controlled steep slopes, deformed drifts atop basement elevations, and the development of thick contouritic piles. Dove Basin is an example of a basin without mounded, plastered or mixed hybrid drifts in the transition between the lower slope and the deep basin, because the upper boundary of the deepest water mass —the Weddell Sea Deep Water— flows shallower along the middle slope. This fact underlines the relevance of the position and depth of water masses in shaping the morphology of the feet of slopes along continental margins.

* Corresponding author.
E-mail address: francisco.lobo@csic.es (F.J. Lobo).

https://doi.org/10.1016/j.margeo.2021.106598
Received 15 January 2021; Received in revised form 2 August 2021; Accepted 4 August 2021
Available online 11 August 2021

1. Introduction

The interaction of down- and along-slope processes in deep-water settings is a relatively common phenomenon, yet because the resulting deposits may exhibit similar sedimentological and morphological features, distinguishing between them may not be straightforward. Both processes are well reflected by seismic data, so that the resulting deposits may be categorized as mixed (downslope/alongslope) drift systems (Rebesco, 2005; Faugeres and Stow, 2008). The most common pattern is exemplified by downslope-generated deposits that tend to be pirated by contour currents, generating a large variety of mixed or hybrid deposits that interfinger, imbricate or are laterally associated (Faugères et al., 1999; Faugères and Mulder, 2011; Sansom, 2018; Fonnesu et al., 2020). The most effective interplay of sediment drifts often occurs in turbidity-current supplied systems (i.e., channel-levee systems and deep-water fans) that are reworked by relatively low velocity contour currents (Stow and Faugères, 2008). Drift development may, however, also be conditioned by debrites (e.g., Knutz and Cartwright, 2004), as well as by hemipelagites or glacigenic deposits (Rebesco, 2005).

In different areas around the Antarctic continent supplied by glacial and glacio-marine processes, turbiditic systems with channel-levee complexes fed from shelf sediment input are subsequently reshaped by vigorous contour currents, constructing asymmetric levees and/or lateral mounded drifts (e.g., Escutia et al., 2002; Michels et al., 2002; Rebesco et al., 2002; Kuvaas et al., 2005; Uenzelmann-Neben, 2006; Solli et al., 2008).

In contrast, depositional settings in the Scotia Sea basins are very far from the sediment input derived from glacial and glacio-marine processes, meaning the formation of extensive turbidite sediment bodies is less significant (e.g., Martos et al., 2013) (Fig. 1). The sedimentary infill of the different Scotia Sea basins is mainly composed of contourite sediment bodies that prevailed after the basins were formed by the late Miocene (Maldonado et al., 2006). The influence of bottom currents on deep-water sedimentation patterns increased progressively over time due to the gradual opening of the different basins (e.g., Pérez et al., 2017, 2021). Additionally, Mass Transport Deposits (MTDs) are known to be a main constituent of the long-term sedimentary record of the Scotia Sea basins (Pérez et al., 2016; Somoza et al., 2019), given their proximity to the Scotia Plate active tectonic boundaries and associated seismicity (Fig. 1).

Most of the previous studies in the Scotia Sea basins are based on the interpretation of low-resolution multichannel seismic data; therefore, deep-water sedimentary patterns are only known on generic terms and at long-term late Cenozoic timescales involving millions of years, both in relation with the development of contouritic and mass transport deposition. In contrast, the study of recent and/or present-day deep-water sedimentary patterns has only been conducted in few places, where contourite deposits have been interpreted as the dominant depositional patterns (e.g., Maldonado et al., 2003; García et al., 2016), although local interactions with MTDs have also been reported (Owen et al., 2014). In order to overcome this gap of knowledge involving recent processes and products, Dove Basin shows good potential for the study of late Quaternary interactions between contourite and gravitational processes along the southern boundary of the Scotia Plate (Fig. 1). From an oceanographic standpoint, Dove Basin is located north of Orkney Passage, which constitutes the main gateway through which deep Antarctic waters flow with the highest velocities into the Scotia Sea (Locarnini et al., 1993; Naveira Garabato et al., 2002b; Tarakanov, 2010). In addition, its physiography is very irregular, as the margins are formed by numerous faults; an extinct spreading center occurs in the middle part of the basin and is bounded to the south by the active Scotia-Antarctica plate boundary. MTD development is particularly favored in this setting (Ruano et al., 2014; Pérez et al., 2016), for which reason, a strong interaction between alongslope processes and MTDs could be expected here.

This study is an extension of the work conducted by Pérez et al. (2017) that focused on the long-term tectonic and stratigraphic development of Dove Basin. Our present contribution deals with recent (i.e., late Quaternary) sedimentary processes through the analysis of

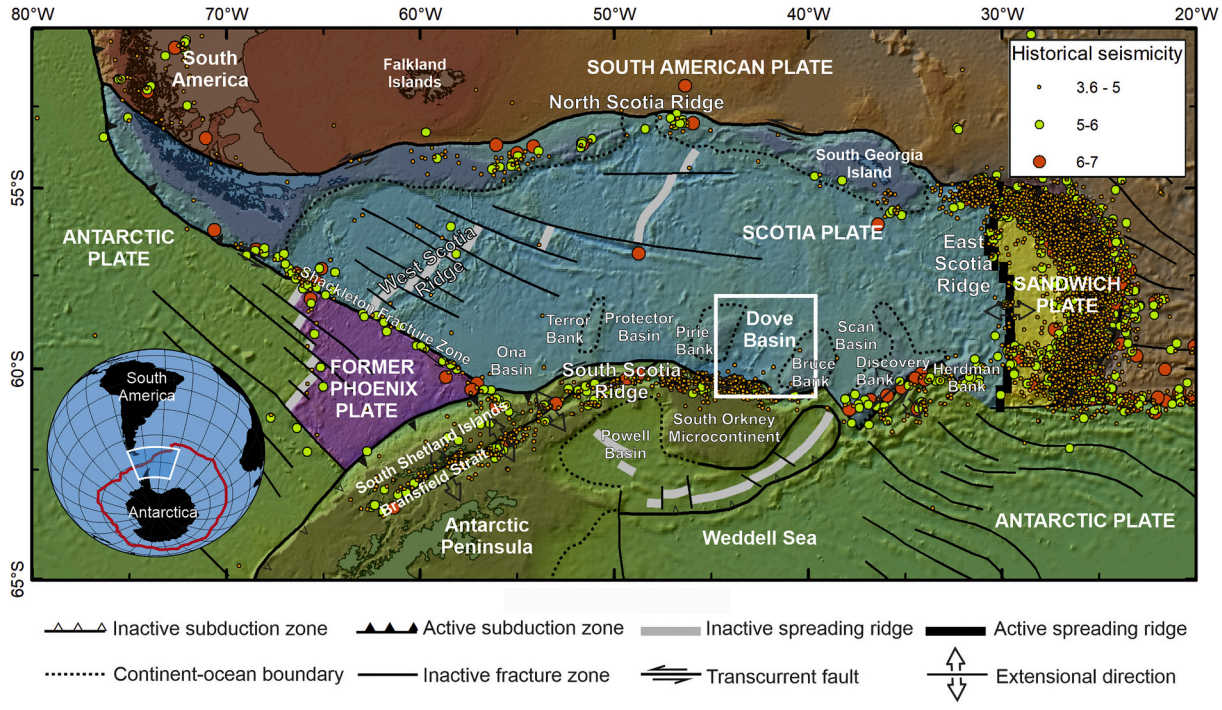

Fig. 1. Geological setting of the Scotia Plate between the South American and Antarctic plates (each plate is highlighted with a different colour), with historical seismicity along the South Scotia Ridge classified according to magnitude. The geographical location of Dove Basin between Pirie and Bruce banks is indicated by a white rectangle. Background bathymetric data extracted from the ETOPO1 1 Arc-Minute Global Relief Model (NOAA National Geophysical Data Center, 2009). Seismicity database extracted from the National Earthquake Information Center (USGS, 2021).

multibeam bathymetric data and high-resolution sub-bottom profiles. We aim to study: (1) the relevance of Dove Basin as an oceanographic conduit for the entrance of Antarctic deep waters from the Weddell Sea into the Scotia Sea as recorded in recent sedimentation patterns; (2) the major types of contourite deposition and the differences with nearby basins; and (3) the role of the basin as an MTD container and the interaction of MTDs with bottom-current processes in the different domains of the basin.

2. Study area

2.1. Geological setting

The Scotia Plate is located between the South American and Antarctic plates, bounded by a complex arrangement of tectonic structures forming the Scotia Arc (Fig. 1). The eastward migration of the arc during the Eocene and Oligocene led to the fragmentation of the continental bridge linking the two continents, hence to their eventual separation (e.g., Lodolo et al., 2006; Eagles and Jokat, 2014; Maldonado et al., 2014). Subsequently, the continental fragments were dispersed along the boundaries of the Scotia Plate (Barker, 2001; Dalziel et al., 2013). Among them, the South Scotia Ridge (SSR) lies along the southern boundary of the Scotia Plate (Fig. 1). The SSR is formed by complex alternations of structural highs and lows developed under a dominant strike-slip tectonic regime. The SSR exhibits a significant seismic activity, and most of the earthquake epicenters are shallow (0–70 km) (e.g., Galindo-Zaldívar et al., 2002; Bohoyo et al., 2007; Lodolo et al., 2010; Civile et al., 2012). North of the SSR, several continental blocks of the ancient bridge separate a number of small basins (Ona, Protector, Dove and Scan, from west to east) (Fig. 1).

Dove Basin is an NNE-SSW elongated oceanic basin of sigmoidal shape extending 200 km N-S and 150 km E-W, bounded laterally by the Pirie (W) and Bruce (E) continental banks (Fig. 1). It contains an elongated high along its middle part, formed by the Dove Ridge and its continuations northward (Dove Seamount) and southward (Galindo-Zaldívar et al., 2014). The central ridge represents the extinct spreading axis, which is bounded by transtensional strike-slip faults, while the marginal banks are bounded by normal faults that individualize structural blocks (Pérez et al., 2017). Different age models have been proposed for the spreading of the basin, either during the late Eocene (Eagles et al., 2006; Barker et al., 2013; Eagles and Jokat, 2014) or during the late Oligocene-early Miocene (Galindo-Zaldívar et al., 2014; Schreider et al., 2018).

2.2. Oceanographic setting

The Antarctic Circumpolar Current (ACC) flows eastward around the Antarctic continent, contributing to its thermal isolation (Rintoul et al., 2001). The ACC comprises several fronts that extend from north to south across the Scotia Sea (Orsi et al., 1995). Of those fronts, the Southern ACC Front (SACCF) and the Southern Boundary of the ACC (SB) extend north of Dove Basin (Fig. 2a). The Circumpolar Deep Water (CDW) propagates freely from west to east in the field of the ACC (Naveira Garabato et al., 2002a; Tarakanov, 2010). The deepest layer of CDW with potential temperatures of 0.2–0.9° is known as the Lower Circumpolar Deep Water (LCDW). The dominant eastward propagation of LCDW exhibits three major pathways; the southernmost path south of the SB crosses Dove Basin from west to east and splits in the middle part of the basin (Tarakanov, 2010) (Fig. 2a).

The deep-water circulation in the Scotia Sea below CDW is dominated by the northward overflow of Weddell Sea Deep Water (WSDW) (Morozov et al., 2010). The WSDW, with potential temperatures below 0.2°, is formed in the Weddell Gyre, which circulates clockwise in the Weddell Sea (Locarnini et al., 1993) above the Weddell Sea Bottom Water (WSBW). The WSDW crosses the SSR through four different gateways (Philip, Orkney, Bruce and Discovery passages, from west to east) (Naveira Garabato et al., 2002b). Orkney Passage, to the east of the South Orkney Microcontinent, is the deepest gateway, where the coldest and most intense WSDW flows northward as a narrow, bottom intensified current with velocities of around 50 cm/s (Locarnini et al., 1993; Naveira Garabato et al., 2002b) (Fig. 2b). Two distinct varieties of WSDW flow over the SSR —an older, warmer and more saline WSDW located deeper in the water column, and a colder, fresher and more recently ventilated WSDW (Naveira Garabato et al., 2002a). These distinct fractions have been referred to as the lower and upper WSDW, the boundary between the two varieties being located at 2000–2500 m water depth along Dove Basin (Tarakanov, 2009). The WSDW branch flowing through Orkney Passage circulates along Dove Basin in an anticyclonic gyre (Naveira Garabato et al., 2002a; Tarakanov, 2009) (Fig. 2b).

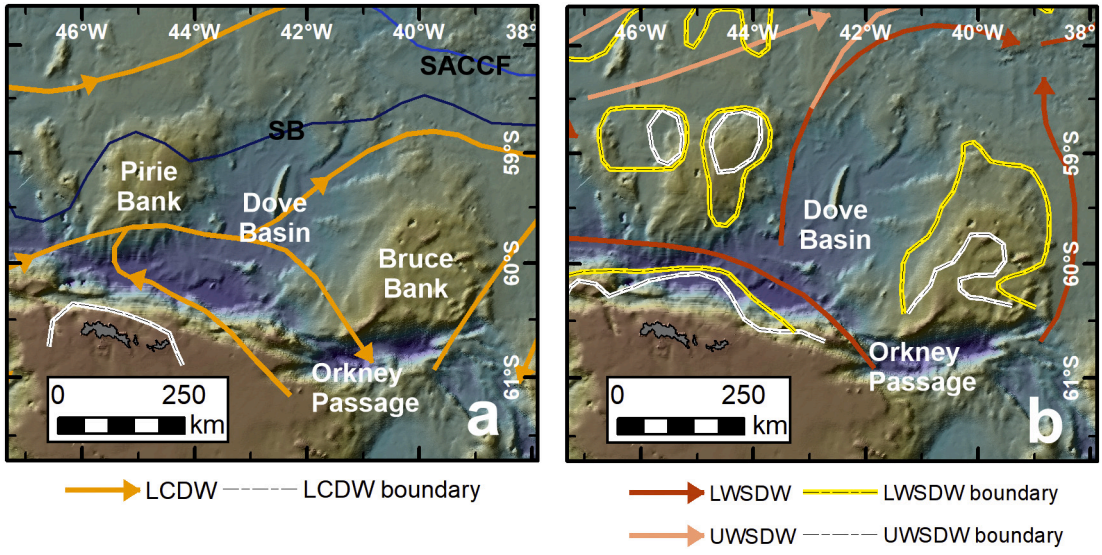

Fig. 2. Distribution of main deep-water masses in Dove Basin. (a) Scheme of circulation of the Lower Circumpolar Deep Water (LCDW) and location of the fronts of the Antarctic Circumpolar Current (ACC) in Dove Basin (after Tarakanov, 2010). Nomenclature of ACC fronts: SACCF: Southern ACC Front; SB: Southern Boundary of the ACC. (b) Scheme of circulation of the Weddell Sea Deep Water (WSDW) in Dove Basin (after Tarakanov, 2009). Legend: LWSDW: lower WSDW; UWSDW: upper WSDW. Background bathymetric data extracted from the 15 arc-second GEBCO 2020 bathymetric grid (GEBCO Compilation Group, 2020).

Hydrographic sections reveal that the shallow parts of the morphological highs surrounding Dove Basin are under the influence of the southernmost path of LCDW (Fig. 3), as suggested by Tarakanov (2010). Below, most of Dove Basin is occupied by the lower WSDW (LWSDW), whereas the boundary with the upper WSDW (UWSDW) deepens to the north (Tarakanov, 2009).

2.3. Deep-water sedimentation patterns

The Cenozoic sedimentary record of the Scotia Sea basins is characterized by several seismic units, pertaining to two distinct intervals (Maldonado et al., 2006). The older units developed during the process of rifting and seafloor spreading, and they show frequent mass transport and turbidite deposits. The younger units overlie a high-amplitude, regionally continuous reflection assigned a late Miocene age (Pérez et al., 2021). These younger units contain abundant evidences of sediment drift development under the combined influence of the ACC and the WSDW (Maldonado et al., 2003; Pérez et al., 2017). Intercalations of contourite deposits with MTDs are also abundant in these younger units north of the SSR, and MTD origins have been related to tectonic and earthquake activity in the nearby plate boundary (Ruano et al., 2014; Pérez et al., 2016). The most recent seismic unit occurs above reflector a', recently dated as late Quaternary in age (i.e., ≈0.4 Ma) (Pérez et al., 2021).

A progressive change from downslope- to alongslope-influenced sedimentation has been documented in the long-term sedimentary record of Dove Basin (Pérez et al., 2017). MTDs also underwent a substantial increase in abundance (Ruano et al., 2014; Pérez et al., 2016). However, the interaction between alongslope and downslope processes during the late Quaternary has not been studied in Dove Basin.

3. Methodology

3.1. Database

The data used in this study comprises a set of high-resolution marine geophysical and hydrographic data (Fig. 4). Geophysical data include multibeam bathymetric data and topographic parametric sub-bottom (TOPAS) profiles, with ancillary multi-channel seismic data.

Multibeam bathymetric data were obtained during the SCAN 2001, SCAN 2004 and SCAN 2008 geophysical surveys onboard RV Hespérides. The SIMRAD EM 12S and EM 120 echo sounders were set up at an operating frequency of 12 kHz and swath apertures of 90 to 120°, providing vertical resolutions of 0.1–0.4 m. Multibeam data used for this study provide about 43% of coverage in Dove Basin. Multibeam files were post-processed with NEPTUNE™ software. Postprocessing of bathymetric data included manual data cleaning to remove erroneous soundings and outlier points. Grids were created with GMT (Generic

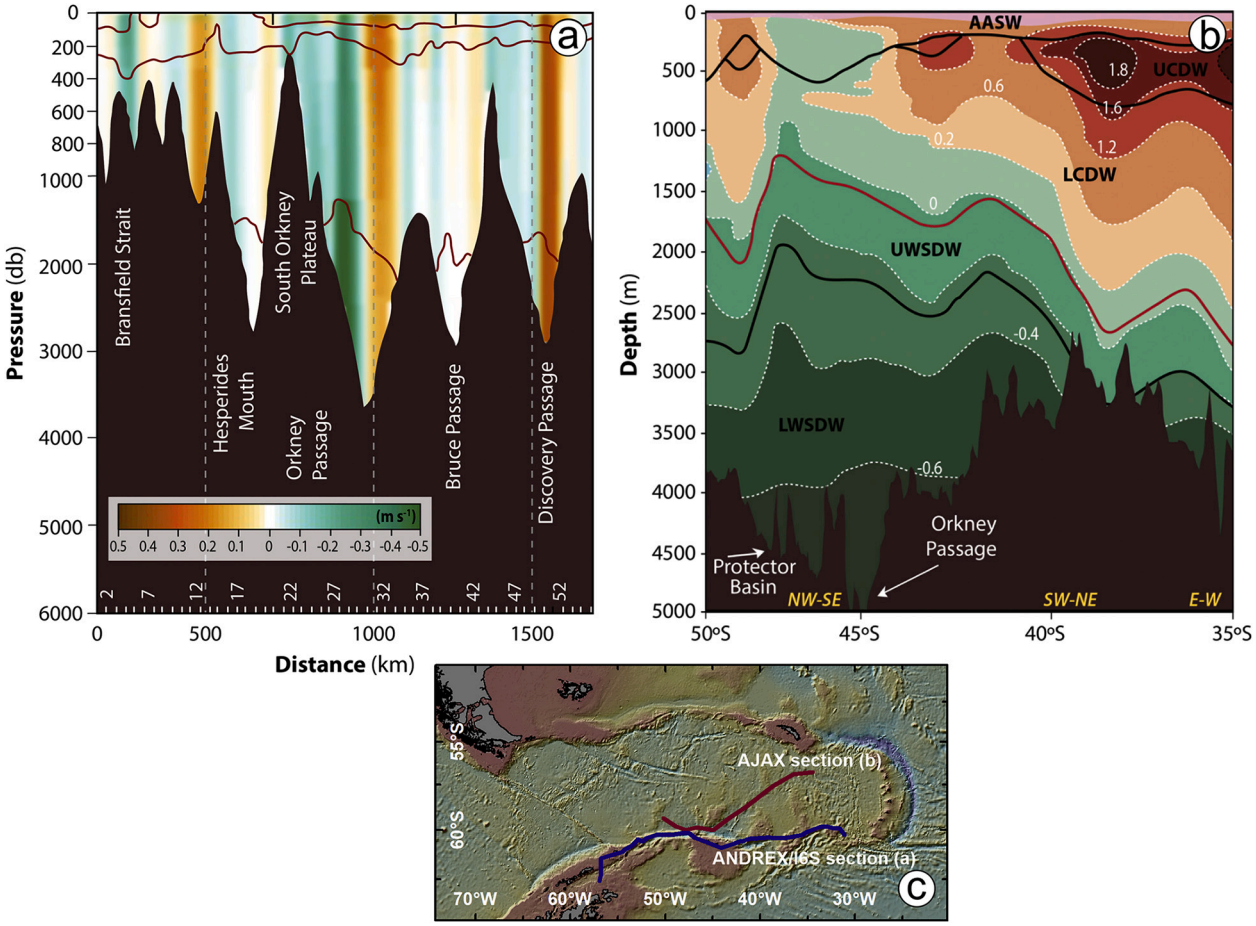

Fig. 3. Hydrographic characterization of key oceanographic transects for Dove Basin. (a) Geostrophic velocities of a segment of the ANDREX/I6S hydrographic section along the South Scotia Ridge (location indicated in c), with positive (negative) values indicating southward (northward) flows (modified from Jullion et al., 2014). The highest northward velocity values occur across Orkney Passage, located south of Dove Basin; (b) hydrographic structure of the water column as defined by the potential temperature along a segment of the AJAX hydrographic section (location indicated in c), which obliquely crosses Dove Basin (simplified from Tarakanov, 2009). Solid bold lines indicate the boundaries between water masses. The boundary between Circumpolar Deep Water (CDW) and Weddell Sea Deep Water (WSDW) is highlighted in red colour. (c) Geographical location of sections a and b. (For interpretation of the references to colour in this figure legend, the reader is referred to the web version of this article.)

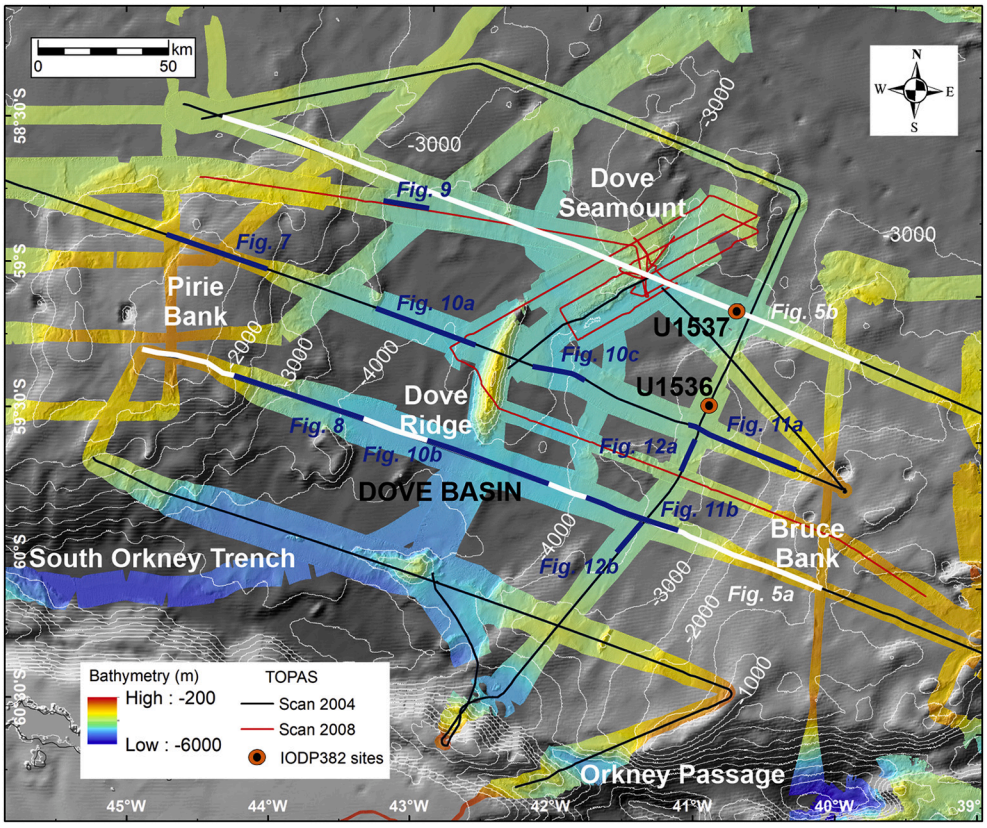

Fig. 4. Geographical location of data used in this study with reference to Dove Basin, including multibeam bathymetric coverage and sub-bottom topographic parametric (TOPAS) profile transects. Major geomorphological features are indicated. The locations of two multi-channel seismic sections crossing the basin are highlighted in white, whereas the locations of sub-bottom profile examples are highlighted in blue colour. The location of drilling sites U1536 and U1537 collected during IODP Expedition 382 is also marked. Background bathymetric data extracted from the 15 arc-second GEBCO 2020 bathymetric grid (GEBCO Compilation Group, 2020). (For interpretation of the references to colour in this figure legend, the reader is referred to the web version of this article.)

Mapping Tools) software; xyz clean data were gridded with block-median and surface GMT commands. Bathymetric grids with a 50 m cell resolution were interpreted using ArcGIS™ software (Fig. 4). To fill the gaps of the multibeam data coverage, we used a 15 arc-second bathymetric grid (GEBCO Compilation Group, 2020).

Nearly 3000 km of acoustic sub-bottom profiles collected in the SCAN 2004 and SCAN 2008 surveys with a TOpographic PArametric Sonar PS 18 (TOPAS™) system were used in this study (Fig. 4). Sub-bottom data were acquired operating in Chirp mode sweeping between two different frequencies: 1.5 and 5 kHz. Pulse length was 20 ms and shooting interval was 5000 ms. Recorded signal length was of 300 ms with a sampling frequency of 35,087 Hz. The Chirp signal was deconvoluted and filtered with a 1 kHz high-pass filter; also, different time-variable gain ramps were applied during acquisition. Post processing included spike removal and noise attenuation using Radexpro™ software. For time-to-depth conversions in sub-bottom profiles, a standard velocity of 1500 m/s was used. Signal penetration is variable in the study area —though values of tens of meters are common, they may locally reach over 100 m. Those thickness values are in agreement with a late Quaternary age (i.e., deposits above reflector a') (Pérez et al., 2021). Sub-bottom profiles were imported to IHS Kingdom™ software for visualization and interpretation purposes.

Two multichannel seismic lines collected in the SCAN 2004 survey crossing the basin were used to correlate the uppermost seismic horizon with sub-bottom acoustic profiles and to highlight the underlying control of deep geological structures on the morphology of recent sedimentary features (Fig. 5). Seismic profile acquisition and processing details are provided in previous studies (Galindo-Zaldívar et al., 2014; Pérez et al., 2017).

Hydrographic data extracted from the World Ocean Atlas 2018 (Boyer et al., 2018) using Ocean Data View™ software (Ocean Data View, 2020) were used to create joint hydrographic and seismic cross sections. Due to the lack of synoptic hydrographic sections, we constructed cross-basin sections by combining all available CTD stations and projecting water sample stations onto the seismic cross sections at distances of up to 50 km. The fields were smoothed to better represent time-averaged distributions to reduce noise related to variations in water mass distributions. This approach provided a regional dataset large enough to suppress small-localized features and seasonal events. The projection distance provided sufficient resolution for clearly identifying regional changes in the hydrographic profiles. Two hydrographic panels crossing Dove Basin with a WNW-ESE trend were constructed. A multibeam bathymetric section (Profile_H01) crossing Dove Ridge was merged with hydrographic data to highlight the water column structure in the middle part of the basin. The southern panel is located south of Dove Ridge, where the multichannel seismic profile SC03 was combined with hydrographic data (temperature, salinity and dissolved oxygen).

3.2. Morpho-stratigraphic interpretation

Recent studies in Dove Basin have provided age constraints for the post-late Miocene sedimentary record of Dove Basin based on the correlation between drilling sites U1536 and U1537 collected during IODP Expedition 382 (Fig. 4) and low-resolution multichannel seismic profiles (Pérez et al., 2021). As a result, four main basin-wide seismic horizons have been defined (Fig. 5). Reflector-a' is the uppermost seismic horizon and has an estimated late Quaternary (i.e., ≈ 0.4 Ma) age (Pérez et al., 2021). We used available multichannel seismic data and extended the interpretation of reflector-a' to our high-resolution sub-bottom profile dataset as much as possible. Due to limitations in data coverage, reflector-a' could be followed over most of the eastern part of the basin; the recognition of reflector-a' west of Dove Ridge was much more uncertain.

The main sub-surface morpho-sedimentary features of Dove Basin (mostly defined above reflector-a') were mapped, taking into account the morphological character observed in bathymetric data and the acoustic facies imaged in the sub-bottom profiles (Fig. 6). To interpret contourite features, major subdivisions of contourite depositional and

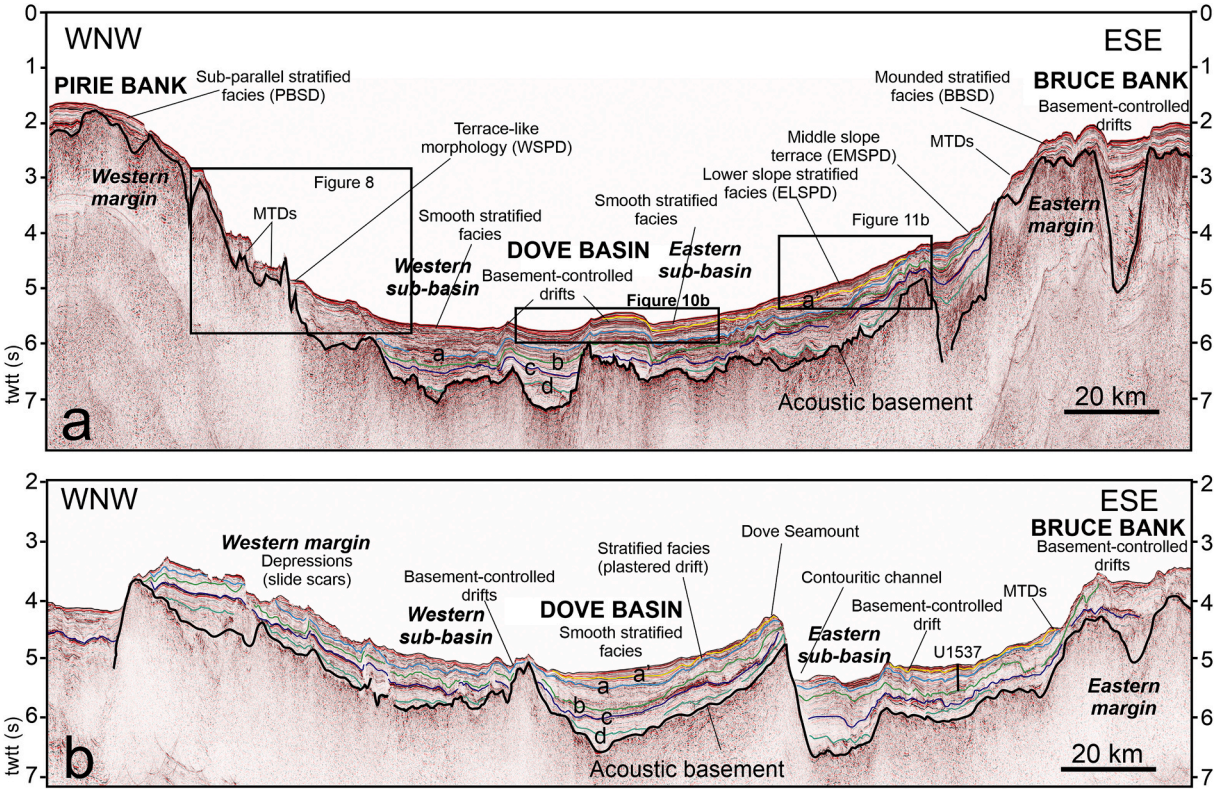

Fig. 5. Examples of multichannel seismic profiles crossing Dove Basin and exhibiting the influence of deep structures on the surface geomorphology: (a) seismic section in the middle part of the basin south of Dove Ridge, where recent deposition is dominated by extensive drifts on the basin slopes, whereas in the central plain sheeted drifts and drifts deformed above basement highs are common. The location of sub-bottom profiles in Figs. 8, 10b and 11 is shown; (b) seismic section in the northern part of the basin crossing Dove Seamount, characterized by the widespread occurrence of basement-controlled drifts and mass movements on the basin slopes. Major seismic horizons (reflectors d, c, b, a and a') defined in the Cenozoic sedimentary record of the basin are depicted (Pérez et al., 2017). Age intervals (in Ma) of seismic horizons (Pérez et al., 2021): Reflector-d age is unresolved; Reflector-c: >8.4; Reflector-b: 3.3–4.8; Reflector-a: 1.2–1.8; Reflector-a': 0.4–07. Location of site U1537 is indicated in the eastern sub-basin (Fig. 5b). Legend: PBSD: Pirie Bank Sheeted Drfit; WSPD: Western Slope Plastered Drift; ELSPD: Eastern Lower Slope Plastered Drift; EMSPD: Eastern Middle Slope Plastered Drift; BBSD: Bruce Bank Sheeted Drift; MTDs: Mass-Transport Deposits. The location of multichannel seismic profiles is indicated in Fig. 4.

erosional features were determined (Faugères et al., 1999; Faugères and Mulder, 2011; Rebesco et al., 2014). In this study, we use the term basement-controlled drift as a generalization of the fault-controlled drift type, which is included in recent contourite classifications (e.g., Rebesco et al., 2008; Rebesco et al., 2014). Specifically, basement-controlled drifts are regarded as sediment drifts whose morphology is determined to some extent by underlying basement structures (Fig. 5). The interpretation of mass movements was based on previous descriptions of related geomorphological features and deposits in high-latitude settings, such as MTDs and gravity-driven erosional features (e.g., Forwick and Vorren, 2007; Masson et al., 2010; Baeten et al., 2013; Laberg et al., 2014).

The observed morpho-sedimentary features were mapped at a regional scale (Fig. 6), considering widely spaced acoustic sub-bottom profiles and multichannel seismic data (Fig. 4). Bathymetric fingerprints of recent morpho-sedimentary features were also included, based on bathymetric data of variable resolution. The maps are therefore limited by the density and nature of the data, resulting in three types of spatial representation: (1) large-scale physiographic features and major sedimentary features were laterally correlated; (2) sedimentary features of limited distribution with outstanding bathymetric expression were mapped along the multibeam bathymetric coverage stripes; (3) sedimentary features without a bathymetric footprint were mapped along the acoustic sub-bottom profiles. Water depths are indicated as meters below sea level.

4. Recent morpho-stratigraphy of Dove Basin

4.1. Sub-bottom acoustic facies and seafloor morphological patterns

The observations are separated taking into account the large-scale physiography of the basin, and three major domains are considered: Pirie Bank/western margin, central basin, and Bruce Bank/eastern margin. In the central basin, a central ridge separates two sub-basins.

4.1.1. Pirie Bank and the western margin

The top of Pirie Bank is characterized by a relatively smooth morphology with sub-parallel stratified facies, having maximum thickness values observable in sub-bottom profiles of around 75 m (Figs. 5a, 7). Several elongated depressions occur around the top of the bank, particularly in the northern part (Fig. 6). The depressions exhibit a dominant NE-SW trend, although their paths are slightly sinuous. The longest depressions are over 15 km long. They show V-shaped cross-sections, with maximum thalweg depths less than 50 m (Fig. 7).

Irregular depressions with semi-circular, amphitheater-shaped plan-view morphologies cover large extents of the slope (Figs. 5b, 6). The heads of the depressions are several kilometers wide. Downslope, different generations of arcuate depressions are observed elsewhere. In cross-sections, depressions exhibit abrupt slopes with no acoustic signal penetration and/or semitransparent acoustic facies (Fig. 8).

Bathymetric highs extend laterally over tens of kilometers on the slope of Pirie Bank (Fig. 6). Most of these highs are highly reflective and exhibit mounded external morphologies (Fig. 8), and occur in front of

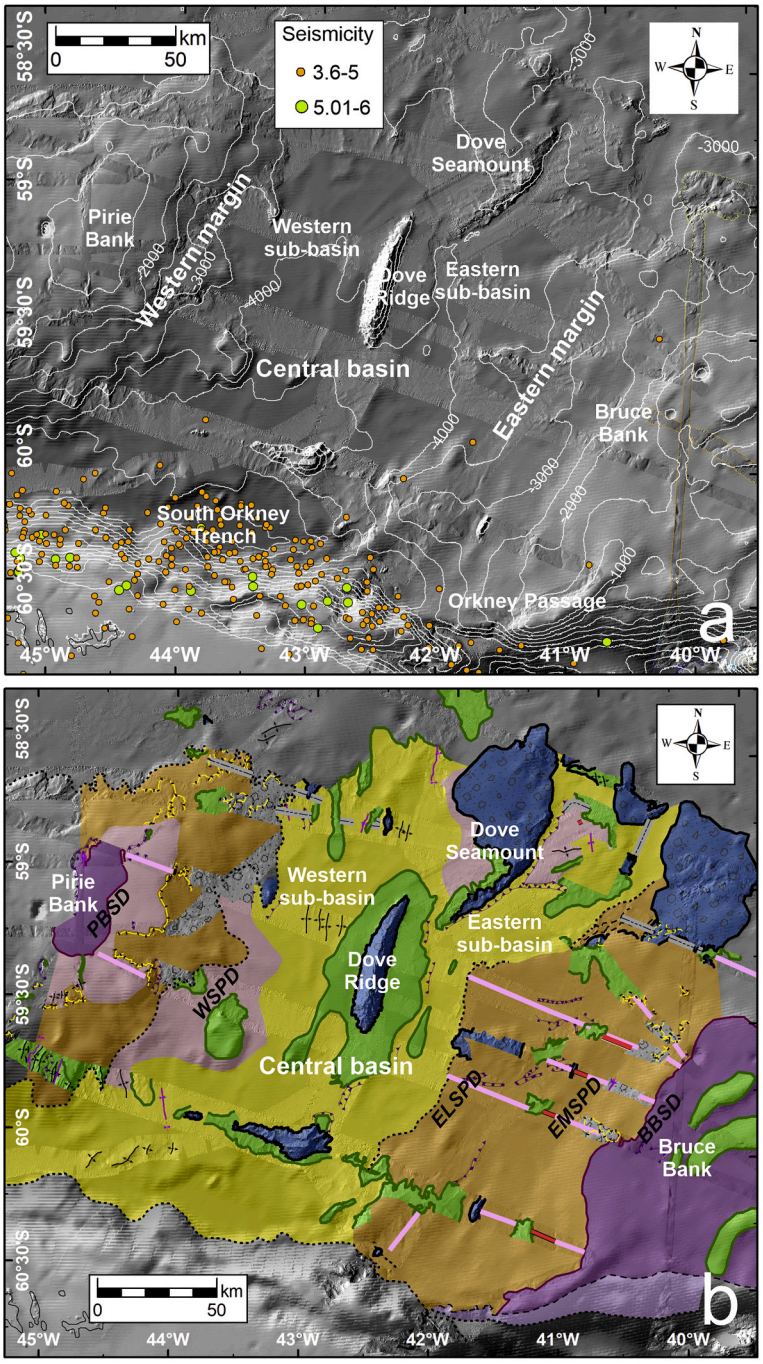

Physiographic features

- Top of bank
- Bank-basin slope boundary
- Basin slope
- Foot of basin slope
- Deep areas (central plain & trench)
- Slope break
- Steep surface

Depositional features

- Plastered drift (PD)
- PD (in seismic section)
- Basement-controlled drift—BCD (generic bathymetric high)
- BCD external boundary
- Elongated ridge crest
- Contouritic terrace
- Mass-transport deposit (MTD)
- MTD (in seismic section)

Erosional & structural features

- Basement outcrop
- Basement outcrop boundary
- Slide scar

Channels (turbiditic or contouritic)

- Channel axis
- Channel boundary

Fig. 6. Geomorphological interpretation of Dove Basin. (a) Uninterpreted geomorphological map of the study area, with hill-shaded multibeam bathymetric data illuminated from the northwest superimposed on the 15 arc-second bathymetric grid (GEBCO Compilation Group, 2020). Epicenters of historical seismicity are superimposed. Seismicity database extracted from the National Earthquake Information Center (USGS, 2021). (b) Interpretation of major geomorphological features in Dove Basin. Legend: PBSD: Pirie Bank Sheeted Drift; WSPD: Western Slope Plastered Drift; ELSPD: Eastern Lower Slope Plastered Drift; EMSPD: Eastern Middle Slope Plastered Drift; BBSD: Bruce Bank Sheeted Drift.

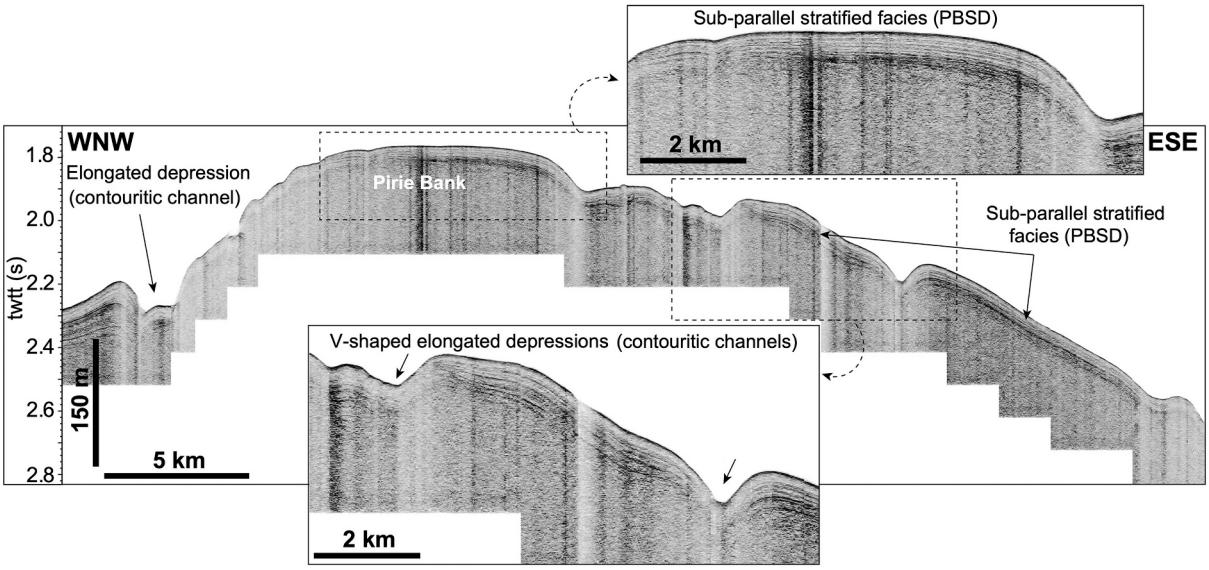

Fig. 7. Acoustic sub-bottom profile crossing the top and uppermost slope of Pirie Bank. Stratified facies and V-shaped depressions are interpreted as contourite features such as the Pirie Bank Sheeted Drift (PBSD) and contouritic channels above it, because of their distribution around and over an isolated basement high and the predominant trend along the isobaths. See location in Fig. 4.

the sets of arcuate depressions (Fig. 6).

Most of the lower slope exhibits a smoother morphological pattern, extending downslope and alongslope for tens of kilometers (Fig. 6). The low-lying deposits are constituted by sub-parallel stratified acoustic facies with intercalated semitransparent sheets/lenses. A terrace-like morphology with a measured slope of 0.5° is locally identified at about 3650 m water depth (Figs. 5a, 8). The thickness of these deposits ranges between 35 and 45 m. Locally, semitransparent lenses stack vertically, amounting to maximum thickness of around 75 m (Fig. 9). At the seafloor, these semitransparent facies produce several irregularly shaped lobes 10–15 km wide with channel-like features on top of them, having maximum depths of 20 m and maximum widths of 2 km (Fig. 9). Several bathymetric elevations tens of meters high are observed in the lower slope (Fig. 6). These highs constitute antiform-like structures composed of stratified reflections (Fig. 8).

4.1.2. *The central basin*

Three sub-domains are defined in the central basin: the western and eastern sub-basins and the central ridge which separates the sub-basins (Fig. 5).

4.1.2.1. The western sub-basin. This part of the basin is constrained

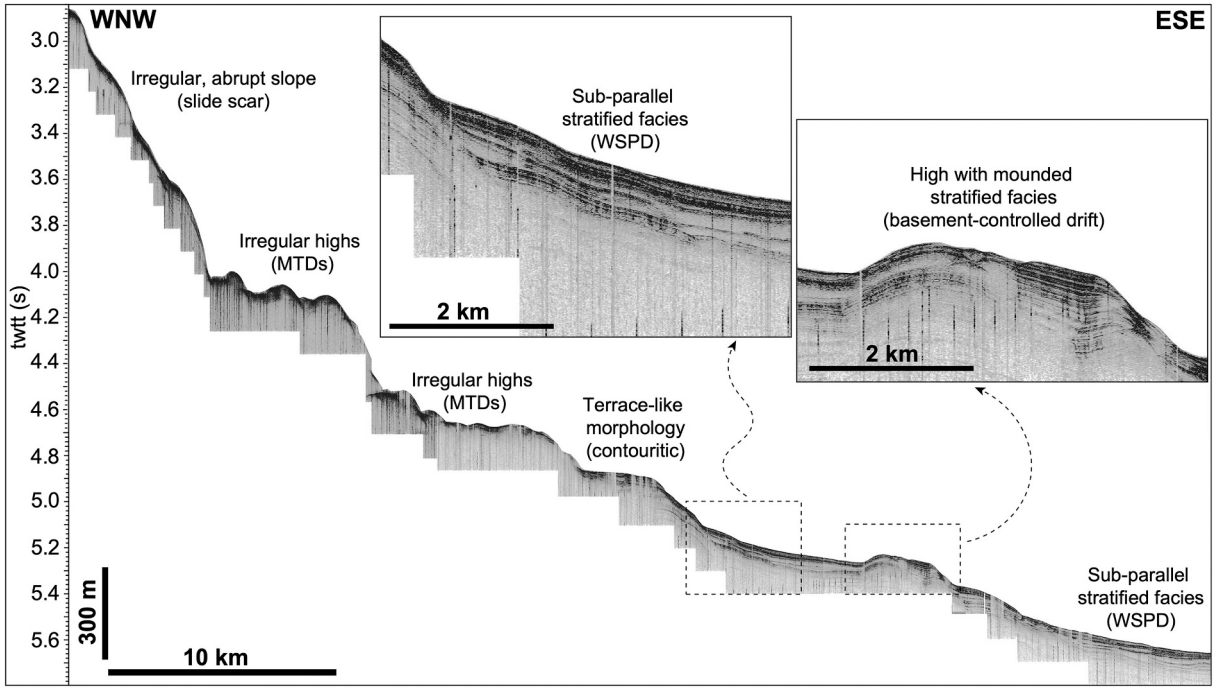

Fig. 8. Acoustic sub-bottom profile crossing the lower slope of the western margin of Dove Basin. To the left, abrupt slopes of slide scars evolve downslope to irregular facies with some hyperbolas, interpreted as the result of mass transport deposits (MTDs). To the right, stratified facies with some intercalated semi-transparent lenses are interpreted as the Western Slope Plastered Drift (WSPD), locally interrupted by a basement-controlled drift. See location in Fig. 4.

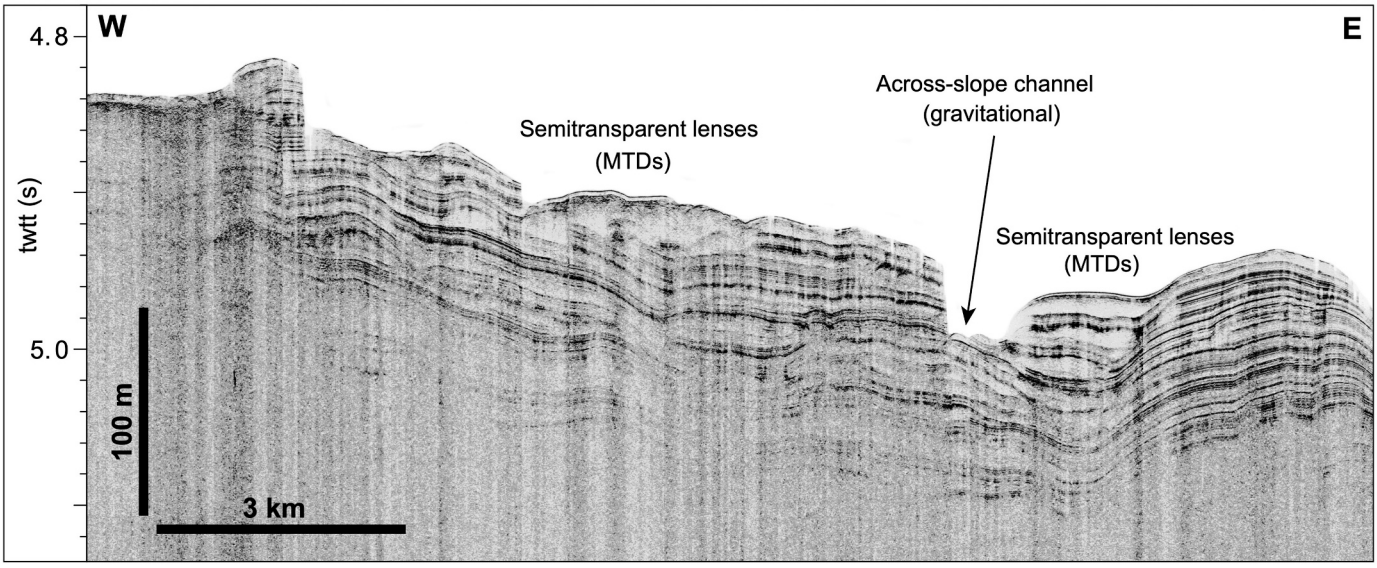

Fig. 9. Acoustic sub-bottom profile at the base of the slope in the western margin of Dove Basin. Semitransparent lenses interpreted as debris flow deposits, a particular type of mass-transport deposit (MTD), are intercalated with stratified facies. These facies are crossed by gravitational channels. See location in Fig. 4.

between the western slope and the central ridge. The western sub-basin exhibits a very smooth, low-lying relief; in the sub-surface, sub-parallel stratified acoustic facies with the local occurrence of semitransparent lenses occur (Figs. 5a, 10a, b). Maximum sediment thickness above reflector-a' is of around 90 m. Several morphologies of kilometric scale are identified; they feature sets of elongated ridges, irregular bathymetric highs, and few elongated depressions (Fig. 6).

Sets of elongated ridges 3–5 km wide and up to 40 m high occur in different parts of the western sub-basin. To the north, these ridges exhibit N-S to NNE-SSW trends, whereas in the southern part of the basin the ridges trend NE-SW (Fig. 6). They exhibit mounded external shapes and are 20–30 m high, with convex-up stratified acoustic facies adapting to underlying highs (Fig. 10a).

Bathymetric highs are larger than the elongated ridges, attaining maximum widths greater than 10 km and maximum heights of about 100 m. Overall, their orientations range from N-S to NNE-SSW, and they show sub-parallel stratified facies overlying older bathymetric highs (Figs. 5b, 10a).

Several types of elongated depressions are identified. A channel almost 3 km wide occurs at the base of the slope, splitting into two branches around a basement outcrop (Fig. 6). Other elongated depressions occur adjacent to morphological highs, showing similar trends and erosive character, and with shallow depths (7.5–15 m) in the channel thalwegs in comparison to the surrounding seafloor.

4.1.2.2. The central ridge. The central ridge includes the aligned bathymetric reliefs of Dove Seamount, Dove Ridge and the WNW-ESE basement elevation south of Dove Ridge (Figs. 5, 6). These highs are surrounded by low-lying sedimentary elevations with flat to mounded tops (i.e., mesa-like morphology) (Fig. 10b). Over most of the area surrounding Dove Ridge, the low-lying deposits exhibit sub-parallel stratified acoustic facies thinning towards their margins, where semitransparent facies are intercalated in the stratified facies (Fig. 10b). Other sedimentary accumulations with interbedded stratified and semitransparent acoustic facies are attached to the western side of Dove Seamount, where they occupy an irregular indentation of the seamount and extend to the north (Fig. 5b).

Several seafloor elongated depressions occur along the eastern side of the central elevations (Fig. 6). A curved channel surrounds a sedimentary mound in the northern part of the southernmost basement ridge. A discontinuous channel runs along the eastern side of the sedimentary accumulation attached to the Dove Ridge (Fig. 5b). It is mostly U-shaped, but locally it exhibits steeper walls with signs of erosion. The channel is partially infilled with sub-parallel stratified facies, including some intercalations of semitransparent lenses (Fig. 10b, c). It is 1.5–2.5 km wide in the southern part and increases to higher widths (around 4 km) in the northern part. Maximum incision depth of the channel is below 40 m. The major channel appears to split into two branches at the southwestern tip of Dove Seamount. The western branch does not show northward continuity, but the eastern branch is very well marked and continuous along the entire length of the Dove Seamount's base, with a mainly NE-SW orientation (Fig. 6). Towards the northeast, this channel exhibits another bifurcation.

4.1.2.3. The eastern sub-basin. The eastern sub-basin has smooth seafloor relief and internal stratified reflections with intercalations of semitransparent lenses (Figs. 5a, 10a). Locally, semitransparent facies occur at the seafloor in the proximity of basement highs. In this sub-basin, the maximum thickness of surficial deposits above reflector-a' is higher (> 150 m) than in the western sub-basin. This general trend is interrupted by several N-S elongated seafloor highs (Fig. 6). Indeed, the northern outlet of the sub-basin is largely blocked by several highs with acoustic responses indicative of a lack of acoustic signal penetration partially or totally covered by stratified mounded deposits.

4.1.3. Bruce Bank and the eastern margin

At the top of Bruce Bank, several elongated highs with broad mounded and stratified patterns can be distinguished between 1250 and 1700 m water depths (Figs. 5, 6). The uppermost slope exhibits an irregular morphology with steep surfaces passing laterally into mounded, semitransparent highs (Figs. 5, 11a) and relatively thin strata (average thickness less than 75 m). The middle slope is marked by a sub-horizontal terrace-like morphology with an average slope of 0.45° shallowing northward from 3100 to 2400 m. Downslope, the middle slope terrace is bounded by a more steeply deepening area with local semitransparent acoustic character, evolving in the lower slope to gently dipping (as low as 1°) sub-surface strata around 150 m thick, with intercalations of semitransparent lenses (Figs. 5a, 11). Maximum sediment thickness above reflector-a' is of about 140 m.

The eastern slope also exhibits diverse seafloor features of kilometric scale, i.e., arcuate to irregular depressions and semitransparent deposits, irregular seafloor highs, and elongated depressions (Figs. 5, 6). Arcuate

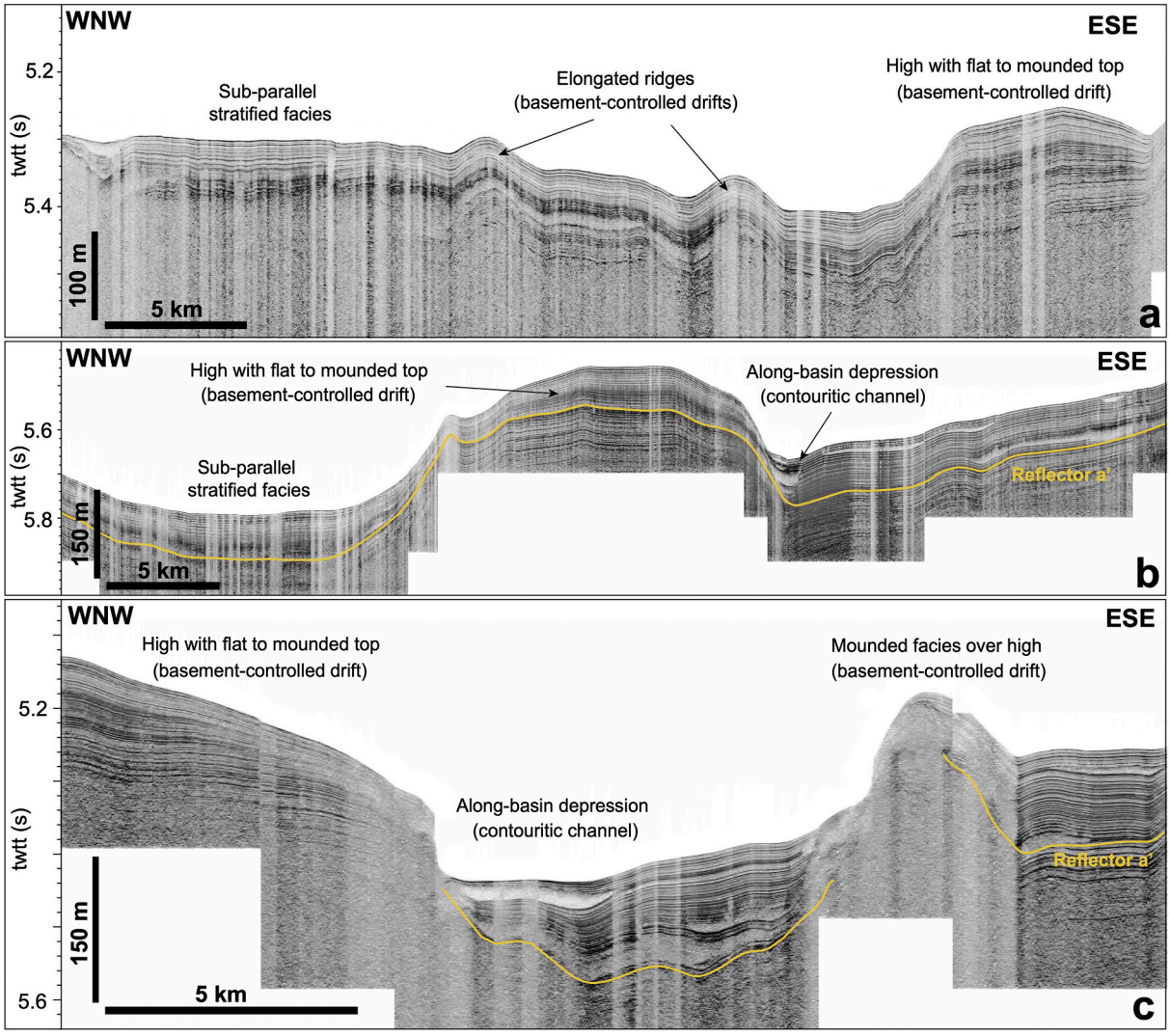

Fig. 10. Acoustic sub-bottom profiles crossing different morpho-stratigraphic elements in the central part of Dove Basin: (a) Section crossing the western sub-basin showing a dominance of stratified facies with constant thickness comprising different types of sediment drifts; (b) Section crossing the central barrier south of Dove Ridge, dominated by a major basement-controlled drift that laterally evolves into stratified facies typical of the central basin; (c) Section crossing the eastern sub-basin mainly depicting the main contouritic channel constrained by basement-controlled drifts. Reflector-a' is interpreted in sections b and c. See location in Fig. 4.

to irregular depressions opening downslope are abundant on the upper slope in the northern part of Bruce Bank, at water depths greater than 1600 m (Fig. 6).

Irregular seafloor highs occur on the lower slope (Fig. 5b). The largest ones (over 10 km wide) exhibit very intricate boundaries in plan view and a preferential W-E trend, with their tops at water depths as shallow as 2500 m (Fig. 6). Some of the highs exhibit mounded reflections at the top, while others do not exhibit acoustic signal penetration (Fig. 12a).

Different types of elongated depressions are found on the eastern margin (Fig. 6). The depressions over Bruce Bank and in the upper slope are 1–2 km wide and up to 70 m deep, exhibit alongslope trends and V-shapes, with truncated reflections at the flanks. In the lower slope, more frequent elongate depressions trend oblique to perpendicular to the slope. They are relatively narrow (1–2 km) and extend tens of kilometers. In cross-section, they are V-shaped and have variable depths of a few tens of meters. They are mostly characterized by semitransparent acoustic responses (Figs. 11b, 12b).

4.2. Changes in acoustic character above and below reflector-a'

Reflector-a' is marked in sub-bottom data by a high amplitude reflection traced through most of the eastern part of the basin. However, its lateral continuity is frequently interrupted by irregular highs. In addition, reflector-a' could not be followed towards the upper part of the slopes, due to the occurrence of highly reflective, erosional features. Acoustic facies tend to be more uniform and with lower lateral continuity below reflector-a'. Above, acoustic facies consist of a well-defined sub-parallel stratified pattern, with alternations of high and low amplitude reflections with high lateral continuity (Fig. 13). In the central basin plain, the subparallel stratified pattern observed in the overlying deposits is interrupted by semitransparent lenses that occur at different stratigraphic levels (Fig. 13a, b). In the eastern slope of the basin, the sub-surface acoustic record above reflector-a' exhibits a higher abundance of semitransparent lenses, that locally stack vertically (Fig. 13c), although stratified facies are dominant laterally (Fig. 13d).

5. Hydrological structure of the water column

Hydrographic profiles across Dove Basin show that the upper part of

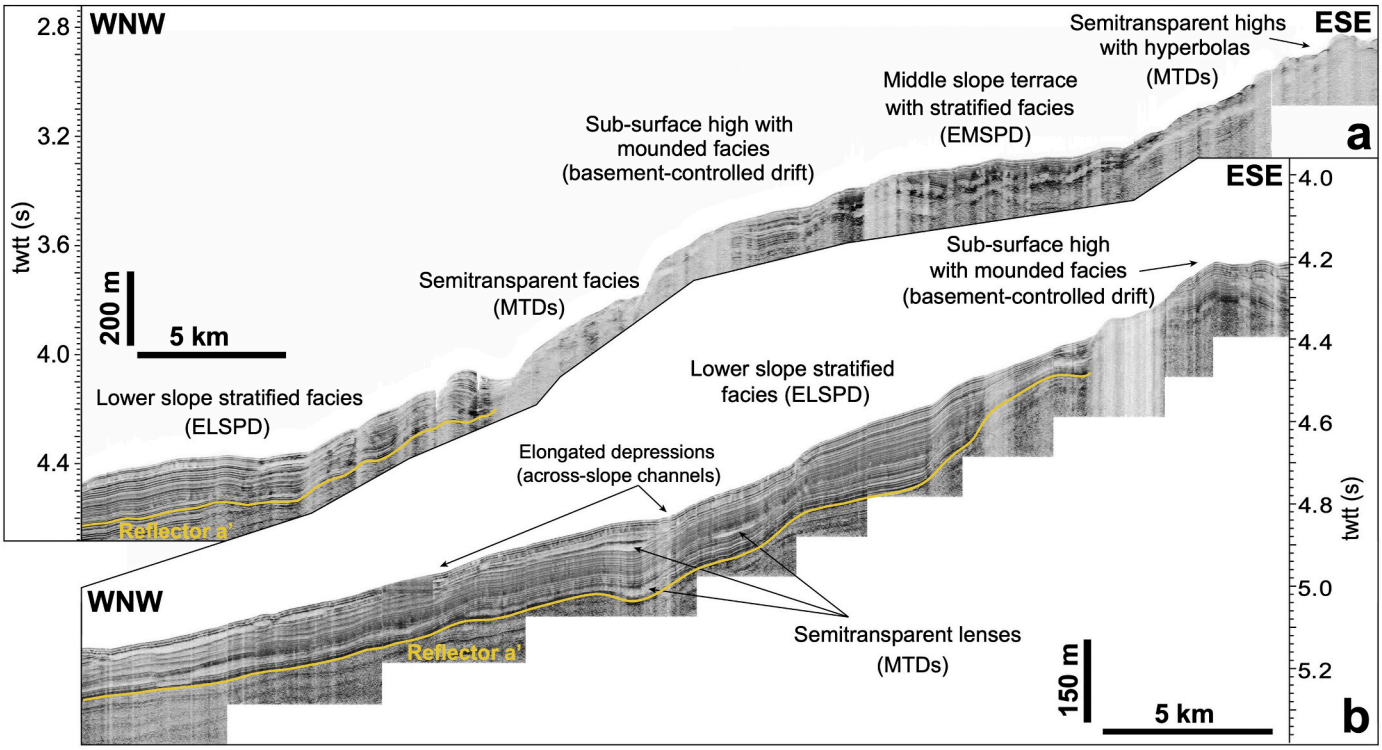

Fig. 11. Acoustic sub-bottom profiles crossing the slope of the eastern margin of Dove Basin: (a) Downslope alternation of mass transport deposits (MTDs) and plastered drifts in the northern part of the eastern slope, such as the Eastern Middle Slope Plastered Drift (EMSPD) and the Eastern Lower Slope Plastered Drift (ELSPD); (b) Stratified facies of the Eastern Lower Slope Plastered Drift (ELSPD) with intercalated semitransparent facies regarded as MTDs. Reflector-a' is partially interpreted in sections a and b. See location in Fig. 4.

the water column is characterized by a sheeted water mass with temperatures higher than 0.5 °C that influences the upper parts of Pirie and Bruce banks at water depths less than 1500–2000 m (Fig. 14). This uppermost part is attributed to the Lower Circumpolar Deeep Water (LCDW).

Below the LCDW, the basin plain is occupied by WSDW (Fig. 14). Within the confines of Dove Basin, at least two main ventilated cores of WSDW with low temperature and high salinity are identified in the eastern sector, adjacent to the slope of Bruce Bank, at water depths of 3500–4000 m (the lower core) and 2500–3000 m (the upper core). In the western part of the basin, a smaller WSDW core is identified along the slope of Pirie Bank, at maximum water depths of 3500 m (Fig. 14).

6. Interpretation of morpho-sedimentary features

The sub-bottom acoustic facies of Dove Basin are primarily characterized by semitransparent facies interbedded with sub-parallel stratified facies. In other deep-water settings around the Antarctic dominated by sediment drifts, such facies successions have been interpreted as the alternating imprint of alongslope bottom-water flows and downslope gravitational flows (Rebesco et al., 2002). A similar overall interpretation is invoked here for the late Quaternary sedimentary record of Dove Basin.

6.1. Banks and basin margins

Sub-parallel stratified facies covering part of the top of Pirie and Bruce banks, and extending downslope to the upper slopes, are interpreted as sheeted drifts (Pirie Bank Sheeted Drift–PBSD and Bruce Bank Sheeted Drift–BBSD) (Fig. 7). Sheeted drifts are a common feature in diverse settings of the Scotia Sea (e.g., García et al., 2016; López-Quirós et al., 2020). These sheeted drifts are locally affected by elongated depressions with a main alongslope trend interpreted as the result of current erosion, and can be regarded as constituting contouritic channels, as in other margins (Howe et al., 1997; Cunningham et al., 2002).

In the western margin, stratified deposits with top horizontal surfaces at the base of the slope are interpreted as a plastered drift —named the Western Slope Plastered Drift (WSPD)— that exhibits intercalated gravity-flow deposits. The bulk of the eastern margin is dominated by sub-parallel stratified facies at two different water depth levels, forming two distinct plastered drifts: the Eastern Middle Slope Plastered Drift (EMSPD), and the Eastern Lower Slope Plastered Drift (ELSPD) (Figs. 6, 11). These plastered drifts would be similar to other sediment drifts reported in the Scotia Sea and the western Falkland Trough (Howe et al., 1997; Owen et al., 2014).

In the western margin, the downslope arrangement of morpho-sedimentary features —ranging from upper amphi-theater-shaped depressions to lower semitransparent deposits— likely portrays a gravitational system with recurrent episodes of sediment failures (e.g., Damuth and Olson, 2001). Similar features area also recognized along the upper slope of the eastern margin, although with lower spatial development (Fig. 11a). Arcuate depressions generating steep slopes evolving downslope to mounded patterns are interpreted as mass transport or slide scars, associated with secondary escarpments and MTDs, resembling the pattern observed elsewhere in the Scotia Sea (Owen et al., 2014; García et al., 2016) and in high-latitude settings (e.g., Forwick and Vorren, 2007; Baeten et al., 2013; Laberg et al., 2014). These facies evolve downslope into acoustically transparent and/or semitransparent acoustic facies interpreted as debris flow deposits (Damuth and Olson, 2001; Owen et al., 2014; Larter et al., 2016); yet here they are regarded as more generic MTDs, which may be intercalated between the slope plastered drifts or stack vertically forming debris fans (Fig. 9).

Channels in the lower slope of the eastern margin (Fig. 12b) or on top of semitransparent fans in the western margin are similar to cross-cutting incisions recognized in areas of debris flow deposit occurrence

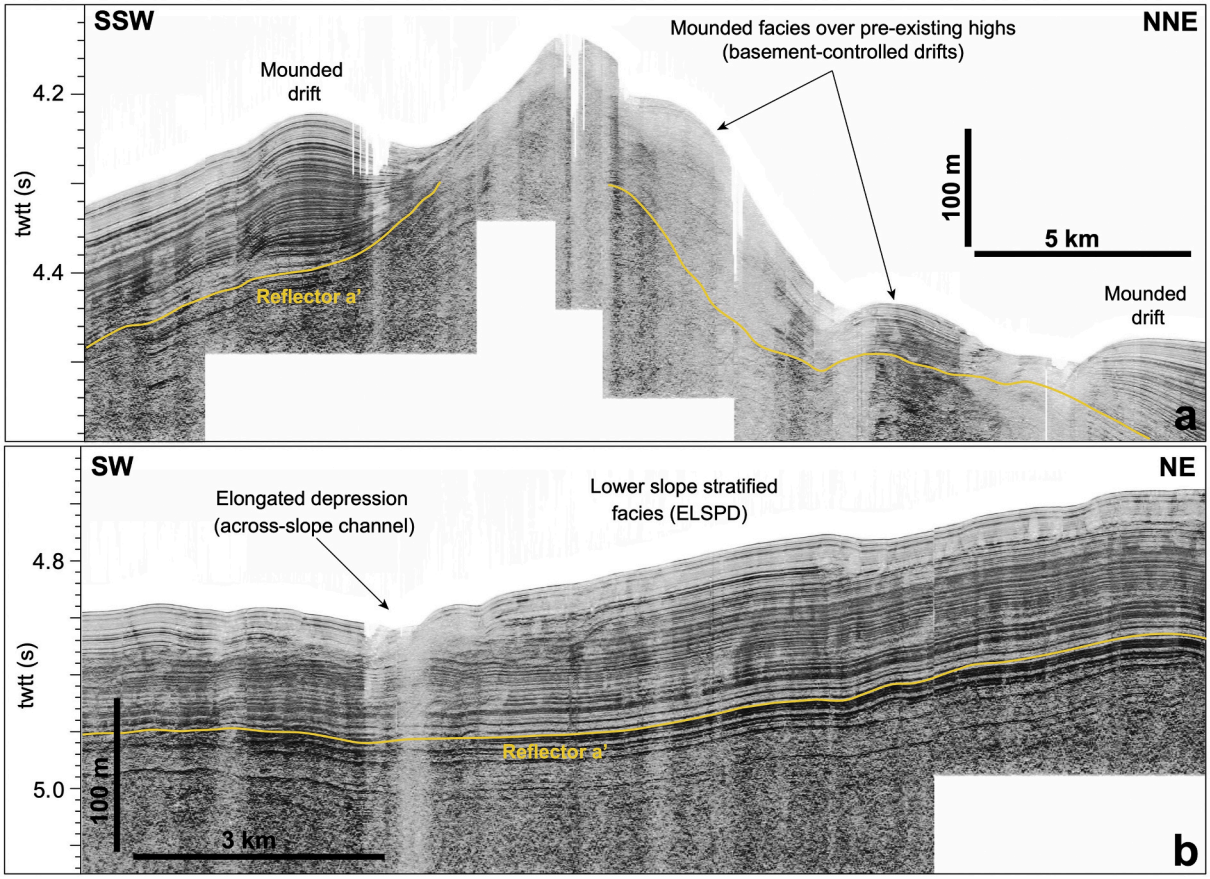

Fig. 12. Acoustic sub-bottom profiles highlighting specific morpho-stratigraphic features in the eastern margin of Dove Basin: (a) Basement-controlled drifts and lateral mounded drifts; (b) Example of across-slope channel with underlying semitransparent facies above a generally stratified slope section, interpreted as a portion of the Eastern Lower Slope Plastered Drift (ELSPD). Reflector-a' is interpreted in sections a and b. See location in Fig. 4.

(Bulat and Long, 2001). These channels could be a result of the transformation of slide masses into low-density sediment flows feeding the lower part of the basin, and they are therefore interpreted as debris flow channels, as observed on other glaciated margins (Bulat and Long, 2001; King et al., 2014).

In both margins, scattered and irregularly distributed mounded highs (Figs. 5, 11), as well as smaller elongated ridges, are interpreted as the result of sediment drift development fostered by underlying structural highs such as anticlines (Bulat and Long, 2001). Indeed, multichannel seismic sections (Fig. 5) reveal that most of these slope elevations are the morphological expressions of deep, faulted basement structures (Pérez et al., 2016, 2017). Therefore, these features are regarded as basement-controlled drifts in the study area. Similar mounded patterns have been recognized in the northern Scotia Sea (Owen et al., 2014). Locally, basement elevations crop out at the surface, developing mounded deposits at their sides interpreted as patch drifts (Fig. 12a). These patterns would indicate a focusing of bottom current flows (Owen et al., 2014). Basement elevations and/or basement-controlled drifts may also favor the local formation of smaller confined drifts or MTDs which, in the lower slope, can be interpreted as debris fans.

6.2. The central basin

The stratified deposits located around most of the central Dove Ridge, with a mesa-like morphology, are regarded as a basement-controlled sheeted drift (Fig. 10b) whose development is driven to some extent by the underlying morphological high (Fig. 5). A similar pattern is detected around the basement high located south of Dove Ridge. In fact, multichannel seismic profiles show that the major seafloor sedimentary elevations observed in the central part of the basin are related in depth to basement morphological highs (Fig. 5). In contrast, Dove Seamount is mainly covered on its western side by a plastered drift, marked by a characteristic decreasing thickness towards shallower water depths. The longest channel identified along the eastern sub-basin is interpreted as a major contouritic channel, whose path is determined by the occurrence of basement highs that constrain the left-hand side of the current (Fig. 6). Indeed, steep erosional walls are typical evidence of the action of intensified contour currents, as suggested for the central Scotia Sea (Maldonado et al., 2003) and other Antarctic contourite systems (Michels et al., 2001).

Most of the remaining central basin stratified facies characterized by relatively constant thickness can be interpreted as sheeted drifts and/or hemipelagic depositions that tend to develop in major seafloor depressions and/or basins (Bulat and Long, 2001; García et al., 2016). In certain places, basement highs would constrain these deposits, which can thus be regarded as confined drifts. Furthermore, mounded drifts laterally associated to channels are locally observed.

Elongated sedimentary ridges and irregular highs scattered in the central basin appear to be controlled by underlying structures (Fig. 5), and are therefore regarded as basement-controlled drifts. Semi-transparent bodies intercalated between the stratified facies next to bathymetric highs are interpreted as debris flow deposits, in a way similar to the margin semitransparent deposits. The channels that follow the main orientation of the basin are regarded as contouritic channels.

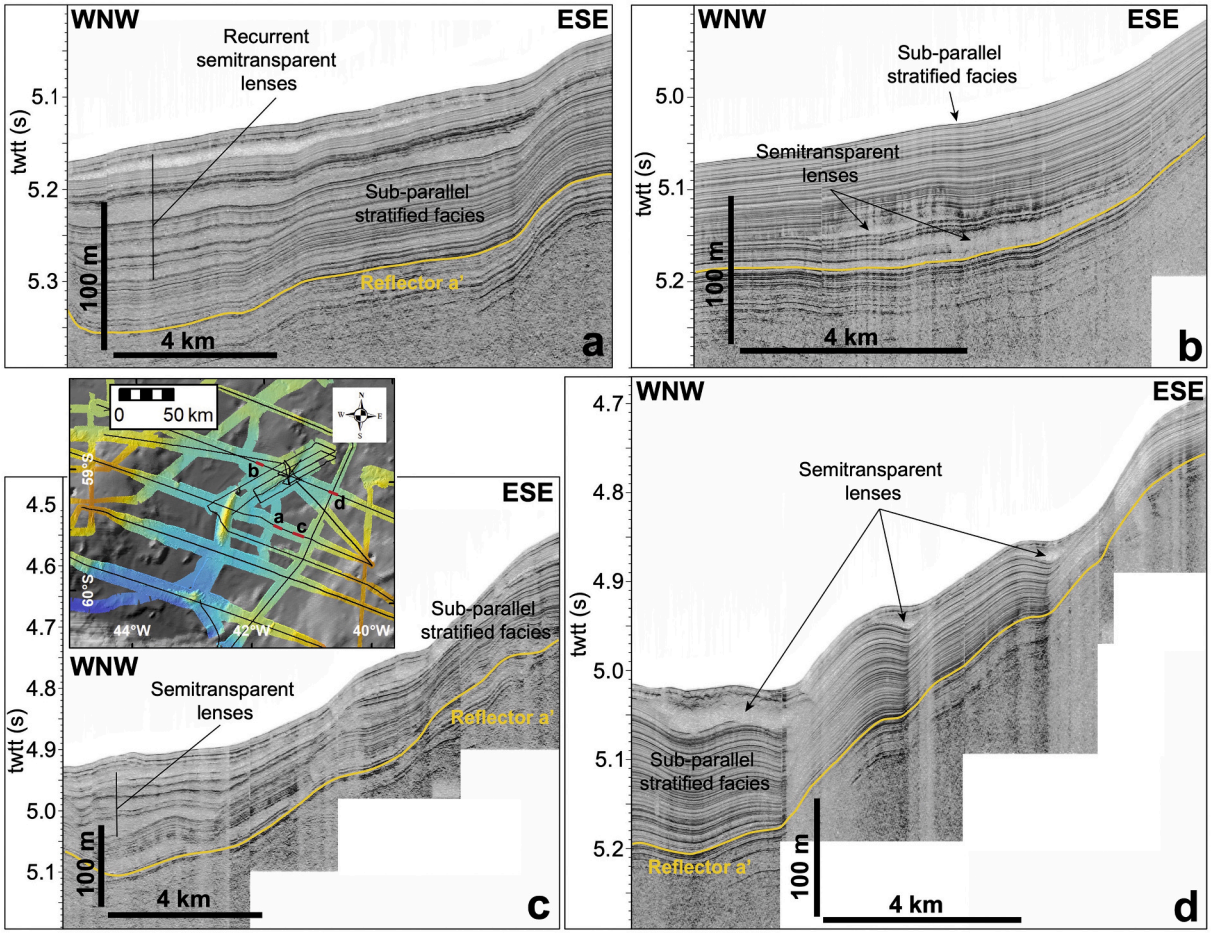

Fig. 13. Examples of seismic facies changes around reflector-a', mostly correlated through the high-resolution sub-bottom seismic data in the eastern part of the basin: (a) High-amplitude, high-continuity sub-parallel stratified facies with several intercalated semitransparent lenses above reflector-a' in the eastern sub-basin. Below reflector-a', seismic facies are less stratified. (b) Occurrence of a semitransparent lens just above reflector-a', buried by a uniform stratified pattern. Below reflector-a', seismic facies are more homogeneous. (c) Alternance of semitransparent lenses and stratified facies over reflector-a', with local stacking of semitransparent lenses, is characteristic of the eastern slope of the basin. (d) Dominance of stratified, undulated reflections with noticeable changes of acoustic amplitudes above reflector-a' in the northern part of the eastern slope.

7. - Discussion

7.1. Elucidating the paths of deep-water flows

Extensive contourite deposition has been identified around much of the Scotia Sea, generically influenced by the ACC and WSDW flows. A latitudinal spatial pattern is observed. In the northern parts of the region, major drifts are generated by the deeper layers of the ACC, such as CDW (Owen et al., 2014; Pérez et al., 2015). In the central Scotia Sea, the complex spatial arrangement of contourite features is attributed to the confluence of the ACC and WSDW flows (Maldonado et al., 2003). In the southern Scotia Sea basins, however, WSDW flows exert a major influence on deep-water sedimentation. The opening of the passages along the SSR during the middle Miocene favored the overflow of WSDW, its progressive strengthening, and the northward displacement of CDW (Pérez et al., 2017, 2021). The influence of ACC flows in the basins of the southern Scotia Sea appear to be largely restricted to the shallower bathymetries of the surrounding banks (e.g., García et al., 2016).

In this framework, Dove Basin is considered to be one of the main conduits guiding the path of the WSDW into the Scotia Sea (Fig. 15a). Most of the basin is occupied by the lower fraction of the WSDW (Tarakanov, 2009), since the basin is located north of Orkney Passage, where the most intense WSDW flows have been documented (Naveira Garabato et al., 2002b; Jullion et al., 2014). Seafloor morphology controls to a large extent the distribution of WSDW in the Scotia Sea, where it flows as a narrow, intense bottom current (Locarnini et al., 1993; Naveira Garabato et al., 2002a).

The most recent low-resolution stratigraphic unit infilling Dove Basin exhibits a tabular shape (Pérez et al., 2017). Our higher resolution analysis of sub-bottom profiles provides information about the regional variability of bottom currents and about the influence of preexisting physiographic traits driving such flows.

The most pronounced contourite features in Dove Basin are located in the eastern sub-basin —including a relatively continuous contourite channel with a lateral drift, the Eastern Lower Slope Plastered Drift (ELSPD). The depth of occurrence (> 3000 m) of the ELSPD would indicate the prevailing influence of the lower WSDW (Tarakanov, 2009). We infer that the main core of the lower WSDW was able to generate the contourite channel on the left-hand side of the current, due to intensification of flow near the physiographic barrier of the central ridge (Fig. 15b). More sluggish current conditions are associated with the formation of plastered drifts (Faugères et al., 1999; Cunningham et al., 2002), such as the ELSPD. We suggest that the interruption and change in orientation of the barrier favors the splitting of its main core into two distinct branches, and finally its exit out of the basin across some of the narrow gaps between basement highs in the northern part of the basin. At a shallower water depth, we tentatively relate the Eastern Middle Slope Plastered Drift (EMSPD) with the major influence of the upper

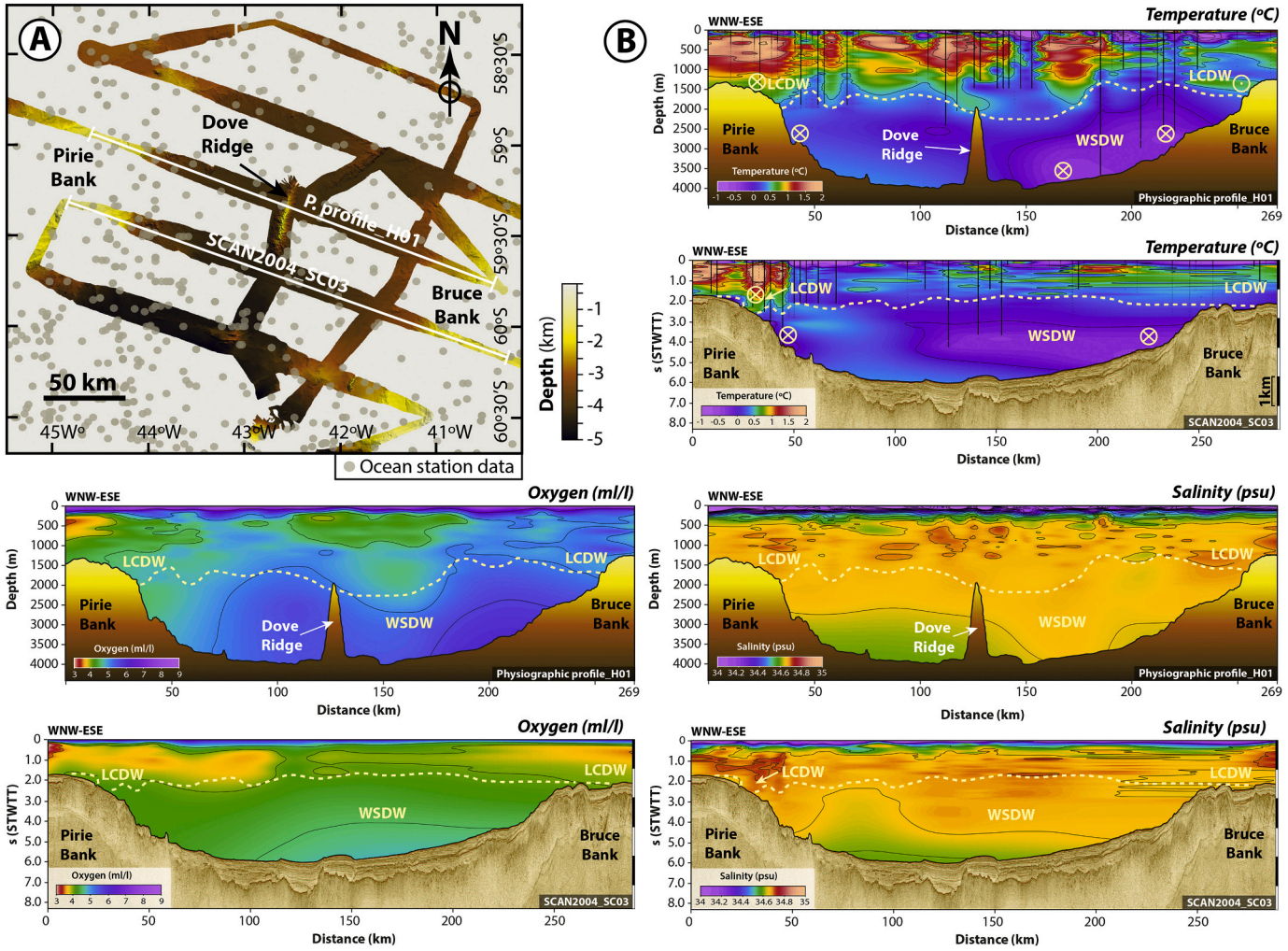

Fig. 14. Hydrographic profiles characterizing water masses in Dove Basin were constructed from hydrographic data from the World Ocean Atlas 2018 (Boyer et al., 2018): (a) Location of cross sections in the middle part of Dove Basin. The northern one (Profile_H01) is combined with a bathymetric profile crossing Dove Ridge. The southern one (SCAN2004_SC03) is combined with a multichannel seismic section located south of Dove Ridge. Stations with available data are represented by grey circles; (b) Panels of temperature (°C), dissolved oxygen (ml/l) and salinity (psu) for the two sections used in this study. Cross sections were constructed by combining all available CTD stations and projecting water sample stations at distances of up to 50 km. The black vertical lines within the water column in the temperature panels show the water depths to which CTDs were lowered.

WSDW (Fig. 15b).

Evidence of contourite deposition is less conspicuous in the western sub-basin. However, the formation of the Western Slope Plastered Drift (WSPD) and its upper terraced surface attest to the influence of the lower WSDW (Fig. 15b), since most of this sub-basin is filled by this water mass and the maximum depth of the water mass core (about 3500 m) corresponds with the water depth of the contouritic terrace.

The different distribution pattern of sediment bodies and occurrence of major sediment drifts at different water depths in the western and eastern sub-basins can be interpreted as the result of the influence of an asymmetric distribution of water masses due to the occurrence of sloping interfaces (Fig. 3b). Under such assumption, most of the western sub-basin would be influenced by LWSDW; in contrast, both components of the WSDW could be able to leave a sedimentary imprint along the eastern basin margin at different water depths.

Additional evidence of contour current action is found on the tops of the lateral banks and adjacent upper slopes. Indeed, the top of the PBSD is influenced by the east-northeast circulation of the LCDW (Fig. 15a) south of the SB (Naveira Garabato et al., 2002a; Tarakanov, 2010). This major trend implies that its influence over the top of Bruce Bank should be more subdued. Such a notion seems to agree with the data presented in this study, as the tabular water mass tongue over the top of the BBSD is interpreted to be the LCDW, which thins to the east. In addition, morpho-stratigraphic evidence of current action in the shallowest part of the Bruce Bank is sparser than over its western counterpart.

7.2. *Unique characteristics of contourite deposition in Dove Basin*

The transition between the present-day lower slope and the continental rise is a common setting for large mounded or plastered contourite drifts (Faugères et al., 1999; Hernández-Molina et al., 2016), whose range of water depths is controlled by the position and circulation of the deepest water mass. Such is the case of basin-scale drifts along the foot of the slope in: a) the South Atlantic (Hernandez-Molina et al., 2009; Preu et al., 2013) due to the influence of the Antarctic Bottom Water; b) along the North Atlantic (Mosher et al., 2017) due to the influence of the North Atlantic Deep Water and Western Boundary Currents; and c) within the South China Sea (Yin et al., 2019) due to bottom water circulation (BW). Large mixed/hybrid drifts are also generated along the feet of slopes (e.g., Tucholke and Mountain, 1986; Locker and Laine, 1992; McGinnis and Hayes, 1995; McGinnis et al., 1997; Escutia et al., 2002; Rebesco et al., 2002). However, in Dove Basin there is no contouritic mound, plastered drift, or mixed/hybrid system in the transition between the present-day lower slope and the deeper basin

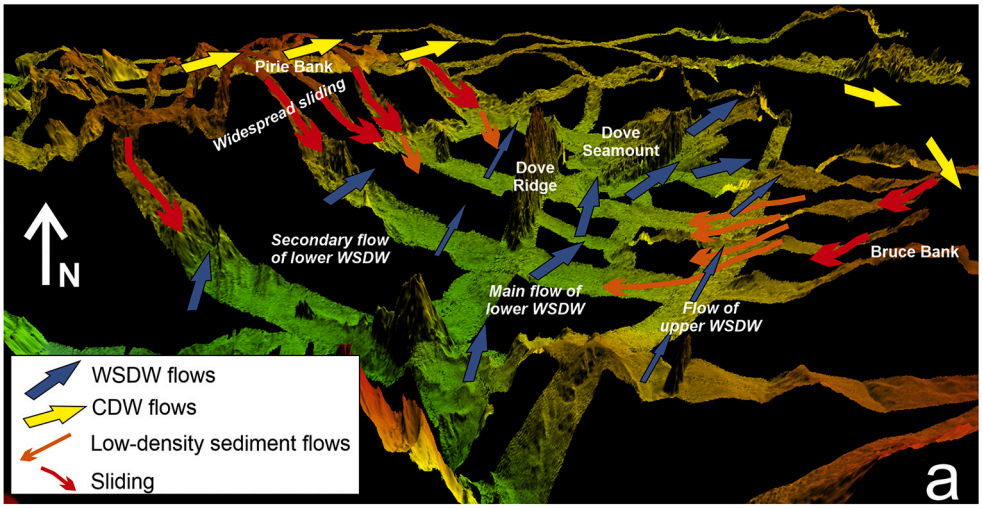

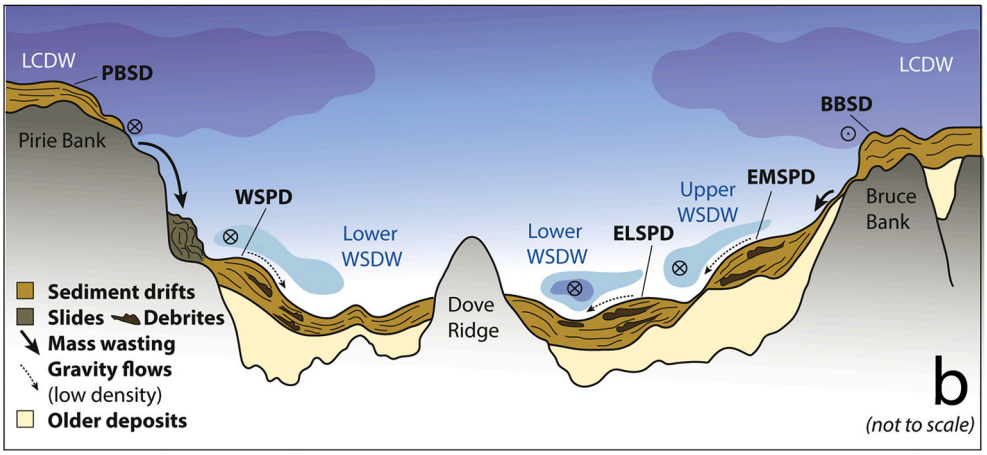

Fig. 15. Summary of processes shaping the morphology of Dove Basin: (a) 3D perspective view of Dove Basin including the major physiographic elements of the basin and lateral banks with schematic depiction of main bottom flows and downslope transport directions in the basin; (b) Schematic cross-section of main sedimentary processes and products revealed during the recent (i.e., late Quaternary) evolution of Dove Basin, highlighting the distinction between the western and eastern sub-basins. CDW: Circumpolar Deep Water; LCDW: Lower CDW; WSDW: Weddell Sea Deep Water; PBSD: Pirie Bank Sheeted Drift; BBSD: Bruce Bank Sheeted Drift; WSPD: Western Slope Plastered Drift; EMSPD: Eastern Middle Slope Plastered Drift; ELSPD: Eastern Lower Slope Plastered Drift.

plain. Here, the top of the deepest water mass —the Weddell Sea Deep Water— is much shallower (Fig. 14) and its circulation generated a basin-scale plastered drift along the middle and lower slope, both in the eastern and western margins, that progressively evolved to sheeted drifts towards the basin plain (Figs. 5, 14).

Previous low-resolution studies conducted in Dove Basin mostly depicted extensive sheeted drifts composing the bulk of the basin infill (Pérez et al., 2017, 2021). However, this study indicates that the most recent sedimentary infill is dominated by plastered and basement-controlled drifts, but mounded elongated drifts are scarce. Plastered drifts are predominantly found in V-shaped troughs characterized by extensive slopes, such as the Falkland Trough (Howe et al., 1997; Cunningham et al., 2002) or the Faroe-Shetland Channel (Bulat and Long, 2001; Damuth and Olson, 2001; Nielsen and Kuijpers, 2018). A similar context can be invoked for Dove Basin: a setting dominated by extensive slopes and relatively reduced deep plains, limited to a large extent by the presence of a central ridge. Ultimately, we propose that the dominance of recent plastered drifts is also indicative of the marked influence of the physiographic and tectonic setting of the basin, in contrast to mounded elongated drifts, which are scarce.

Tectonically controlled drifts have been recognized regionally at specific locations, possibly owing to the tectonic activity and reactivation of previous major faults around the SSR. For instance, numerous basement/tectonic drifts that parallel irregularities of the basement surface have been reported for the northern Weddell Sea (Maldonado et al., 2005). Tectonic drifts are also relatively common in the southern part of Ona Basin, where they tend to grow parallel to basement structures (Martos et al., 2013; López-Quirós et al., 2020).

In Dove Basin, irregularities and structural features associated with the igneous basement have determined a pervasive occurrence of basement-controlled drifts in the central basin and the basin margins. In the central basin, the occurrence of an N-S trending basement high (Galindo-Zaldívar et al., 2014; Pérez et al., 2017) has conditioned the formation of major drifts, as this basement elevation has been a significant barrier for deep-water flows at least since the early-middle Miocene. Additional normal faults are scattered in the central part of the basin, while the marginal banks are affected by many normal faults, most having northern trends inherited from the opening and spreading of the basin (Pérez et al., 2017). The numerous basement-controlled drifts identified in the basin margins, and the smaller drifts scattered in the central basin, exhibit dominant trends that are compatible with the influence of these structures.

7.3. *Widespread alongslope-downslope interactions*

Alternations between alongslope and downslope sedimentation patterns have been reported in several deep-water environments around Antarctica (e.g., Michels et al., 2001; Escutia et al., 2002; Rebesco et al., 2002). Downslope processes result in the formation of distal turbiditic suspended sediment that can be entrained by alongslope bottom currents. MTDs mainly represented by gravity flow deposits are commonly found among early continental margin deposits, and are progressively replaced by channel-levee and drift bodies (Michels et al., 2001, 2002; Escutia et al., 2002).

Dove Basin appears to be an unusual example in comparison with other basins of the Scotia Sea (Ruano et al., 2014; Pérez et al., 2017;

López-Quirós et al., 2020), since the interaction between downslope and alongslope process is not confined to a particular physiographic setting. Instead, it occurs in the margins and the central basin plain, including the basement-controlled drifts associated with the central ridge, the sheeted drifts and the contouritic channels. The interaction has persisted throughout time, and continues to the present day. We discuss different processes that can lead to these temporal alternations indicated by the interlayered stratified and semitransparent facies.

Alternations between downslope and alongslope processes are usually driven by glacial-interglacial cycles (Faugères et al., 1999; Mulder et al., 2008; Faugères and Mulder, 2011). The fact that MTD development seems to increase in frequency above reflector-a' (Fig. 13) would suggest increased influence of glacial cycles during the last 0.4 Ma. However, it seems unlikely that either glacigenic or glacio-marine processes affected MTD development in the deep realm as it has been reported in other Antarctic settings more directly influenced by glacial-interglacial changes in terrestrial supplies (e.g., Lee et al., 2012; Holder et al., 2020; Jimenez-Espejo et al., 2020). In the case of Dove Basin, the basin is distant from continental sediment transport routes and the banks surrounding the basin are rather deep. Minimum depths on the top of the banks are between 1200 and 1300 m, meaning ice sheet grounding would not have been possible during Quaternary glacial periods.

Another possibility would be to consider a periodic reactivation of tectonic structures. Although recent faulting affecting the seafloor or the shallow sub-surface is not observed in the study area, the plate boundary south of Dove Basin is frequently affected by seismic events of magnitude <5 (Fig. 1); the seismic shaking could favor sediment remobilization. In order for the seismic shaking to be effective, an additional preconditioning factor needs to be invoked. We propose that the interactions are fostered by over-steepening, which may have different origins. For example, the influence of normal faulting in basement inheritance of the margins could lead to the formation of steep slopes; this seems to occur preferentially in the western margin, where MTDs mostly comprise extensive slides, producing an overall degraded morphology that seems to be conditioned by the strong influence of basement normal faults (Pérez et al., 2017). In addition, the conspicuous occurrence of basement-controlled drifts, usually related to local high sedimentation rates, can favor local lateral instabilities, particularly in the eastern margin. Finally, around the study area thick recent sediment drifts generating significant reliefs and lateral slopes are locally observed. In contrast, in the upper slope drifts tend to be poorly developed. In fact, this could represent a case where upper slope contourite deposition may also act as a trigger for sediment remobilization (Mulder et al., 2008). Such positive feedback —where the thinning of contourite deposits in upper slopes may favor the activation of gliding planes— has also been observed in the Tyrrhenian Sea slope (Martorelli et al., 2016) and the upper slope of the Norwegian margin (Baeten et al., 2016). In the study area, therefore, continuous gravitational activity would have enabled the establishment of a sediment transfer system between the thinned and cannibalized banks and upper slope drifts, and the thickened and more extensive lower slope drifts. This pattern is also reflected in the late Quaternary architecture overlying reflector-a', since semitransparent deposits interpreted as MTDs decrease in frequency from the basin margins to the central part of the basin (Fig. 13).

8. Conclusions

A pervasive arrangement of stratified and semitransparent acoustic facies in the basin margins and the basin plain of Dove Basin can be attributed to continuous alternation between alongslope and downslope processes that persisted during the late Quaternary.

In Dove Basin, deep Antarctic waters composed of Weddell Sea Deep Water (WSDW) exert a primary influence on sedimentation patterns, with marked differences in the eastern and western sub-basins. The main flows are channeled through the eastern part of the basin, due to the barrier effect caused by a lineation of basement elevations inherited from an extinct spreading center. The main path of the lower fraction of the WSDW is indicated by a nearly continuous contourite channel. Laterally, the recognition of two different plastered drifts at different water depths along the eastern basin slope most likely reflects the influence of the two WSDW fractions. Contourite features are more scarce in the western part of the basin, which could indicate the influence of a different and possibly weaker core of lower WSDW. The influence of the LCDW is limited to the tops and upper slopes of the banks, where stratified sheeted drifts and scattered contourite channels are recognized. Ultimately, the asymmetry is a consequence of the basin physiography and the structure of the water column, due to the existence of sloping interfaces between water masses. This configuration allows the preferential entrance of upper WSDW along the eastern part of the basin.

Dove Basin is distinguished from the neighboring southern Scotia Sea basins and other Antarctic margins by an anomalously high incidence of plastered and basement-controlled drifts, in contrast to the widespread dominance of mounded elongated drifts in other settings. It represents an example of a basin without mounded, plastered or mixed/hybrid systems in the transition between the lower slope and the basin plain. This major difference is attributed to: (a) the strong imprint in the basin physiography of the inherited geology; (b) the vertical structure of water masses, since the fact that the base of slope is occupied by the lower WSDW implies that its top boundary (interface) is shallower along the middle slope, precluding the formation of significant mounded drifts, and thus revealing the important role of the position and depth of water masses in shaping the foot of slope morphology along continental margins.

The continuous interaction between contourite and mass movement processes was favored by over-steepening, yet driven by basement heritage, by the conspicuous occurrence of basement-controlled drifts, and by the occurrence of locally thick sediment drifts. Additionally, seismic activity along the southern plate boundary can foster sediment remobilization. These interactions further reveal temporal and spatial patterns, indicating that styles of contourite deposition may act as preconditioning factors when triggering downslope processes.

Data Availability

Multibeam bathymetric data are available in the International Bathymetric Chart of the Southern Ocean (IBCSO) version 1.0 database (https://www.scar.org/science/ibcso/ibcso/). Sub-bottom parametric TOPAS profiles are available from the corresponding author upon reasonable request. Multichannel seismic data are available in the Antarctic Seismic Data Library System for Cooperative Research (SDLS) (https://www.scar.org/sdls/). Hydrographic data are available in the World Ocean Database 2013 (https://www.nodc.noaa.gov/OC5/WOD13/data13geo.html).

Declaration of Competing Interest

None.

Acknowledgements

Funding for this research was provided by the Spanish Ministry of Science and Innovation (grants CTM2014-60451-C2-1/2-P and CTM2017-89711-C2-1/2-P) co-funded by the European Union through FEDER funds. The research was conducted in collaboration with '*The Drifters Research Group*' of the Royal Holloway University of London (UK), and is also related to the projects CTM 2012-39599-C03, CGL2016-80445-R, CTM2016-75129-C3-1-R and CGL2015-74216-JIN. We thank the commander, officers and crew of the BIO HESPERIDES for their support in obtaining the data, sometimes under severe sea conditions. Jean Sanders reviewed the English style of the manuscript. Rob Larter (BAS, UK) and an anonymous reviewer provided numerous

useful remarks that improved an initial version of the manuscript. Seismic interpretations were made using the IHS Kingdom™ software, thanks to the participation of the *Instituto Andaluz de Ciencias de la Tierra* in the IHS University Grant program.

References

Baeten, N.J., Laberg, J.S., Forwick, M., Vorren, T.O., Vanneste, M., Forsberg, C.F., Kvalstad, T.J., Ivanov, M., 2013. Morphology and origin of smaller-scale mass movements on the continental slope off northern Norway. Geomorphology 187, 122–134. https://doi.org/10.1016/j.geomorph.2013.01.008.

Baeten, N.J., Laberg, J.S., Forwick, M., 2016. Submarine mass movements affecting contourites on the continental slope offshore of the Lofoten Islands, North Norway. In: Dowdeswell, J.A., Canals, M., Jakobsson, M., Todd, B.J., Dowdeswell, E.K., Hogan, K.A. (Eds.), Atlas of Submarine Glacial Landforms: Modern, Quaternary and Ancient, pp. 397–398. https://doi.org/10.1144/m46.41.

Barker, P.F., 2001. Scotia Sea regional tectonic evolution: implications for mantle flow and palaeocirculation. Earth-Science Rev. 55, 1–39. https://doi.org/10.1016/S0012-8252(01)00055-1.

Barker, P.F., Lawver, L.A., Larter, R.D., 2013. Heat-flow determinations of basement age in small oceanic basins of the southern central Scotia Sea. Geol. Soc. London Spec. Publ. 381, 139–150. https://doi.org/10.1144/sp381.3.

Bohoyo, F., Galindo-Zaldívar, J., Jabaloy, A., Maldonado, A., Rodríguez-Fernández, J., Schreider, A., Surinach, E., 2007. Extensional deformation and development of deep basins associated with the sinistral transcurrent fault zone of the Scotia Antarctic plate boundary. In: Cunningham, W.D., Mann, P. (Eds.), Tectonics of Strike-Slip Restraining and Releasing Bends, pp. 203–217. https://doi.org/10.1144/sp290.6.

Boyer, T.P., Garcia, H.E., Locarnini, R.A., Zweng, M.M., Mishonov, A.V., Reagan, J.R., Weathers, K.A., Baranova, O.K., Seidov, D., Smolyar, I.V., 2018. World Ocean Atlas 2018. NOAA National Centers for Environmental Information. Dataset. https://accession.nodc.noaa.gov/NCEI-WOA18.

Bulat, J., Long, D., 2001. Images of the seabed in the Faroe-Shetland Channel from commercial 3D seismic data. Mar. Geophys. Res. 22, 345–367. https://doi.org/10.1023/A:1016343431386.

Civile, D., Lodolo, E., Vuan, A., Loreto, M.F., 2012. Tectonics of the Scotia–Antarctica plate boundary constrained from seismic and seismological data. Tectonophysics 550–553, 17–34. https://doi.org/10.1016/j.tecto.2012.05.002.

Cunningham, A.P., Howe, J.A., Barker, P.F., 2002. Contourite sedimentation in the Falkland Trough, western South Atlantic. In: Stow, D.A.V., Pudsey, C.J., Howe, J.A., Faugères, J.-C., Viana, A.R. (Eds.), Deep-Water Contourite Systems: Modern Drifts and Ancient Series, Seismic and Sedimentary Characteristics, pp. 337–352. https://doi.org/10.1144/gsl.mem.2002.022.01.24.

Dalziel, I.W.D., Lawver, L.A., Norton, I.O., Gahagan, L.M., 2013. The Scotia Arc: genesis, evolution, global significance. Annu. Rev. Earth Planet. Sci. 41, 767–793. https://doi.org/10.1146/annurev-earth-050212-124155.

Damuth, J.E., Olson, H.C., 2001. Neogene-Quaternary contourite and related deposition on the West Shetland Slope and Faeroe-Shetland Channel revealed by high-resolution seismic studies. Mar. Geophys. Res. 22, 369–398. https://doi.org/10.1023/A:1016395515456.

Eagles, G., Jokat, W., 2014. Tectonic reconstructions for paleobathymetry in Drake Passage. Tectonophysics 611, 28–50. https://doi.org/10.1016/j.tecto.2013.11.021.

Eagles, G., Livermore, R., Morris, P., 2006. Small basins in the Scotia Sea: the Eocene Drake Passage gateway. Earth Planet. Sci. Lett. 242, 343–353. https://doi.org/10.1016/j.epsl.2005.11.060.

Escutia, C., Nelson, C.H., Acton, G.D., Eittreim, S.L., Cooper, A.K., Warnke, D.A., Jaramillo, J.M., 2002. Current controlled deposition on the Wilkes Land continental rise, Antarctica. In: Stow, D.A.V., Pudsey, C.J., Howe, J.A., Faugères, J.-C., Viana, A. R. (Eds.), Deep-Water Contourite Systems: Modern Drifts and Ancient Series, Seismic and Sedimentary Characteristics, pp. 373–384. https://doi.org/10.1144/gsl.mem.2002.022.01.26.

Faugères, J.-C., Mulder, T., 2011. Contour currents and contourite drifts. In: Heiko, H., Thierry, M. (Eds.), Deep-Sea Sediments. Elsevier, Amsterdam, pp. 149–214. https://doi.org/10.1016/b978-0-444-53000-4.00003-2.

Faugeres, J.-C., Stow, D.A.V., 2008. Contourite drifts: Nature, evolution and facies. In: Rebesco, M., Camerlenghi, A. (Eds.), Contourites. Elsevier, Amsterdam, pp. 259–288. https://doi.org/10.1016/S0070-4571(08)00214-8.

Faugères, J.-C., Stow, D.A.V., Imbert, P., Viana, A., 1999. Seismic features diagnostic of contourite drifts. Mar. Geol. 162, 1–38. https://doi.org/10.1016/S0025-3227(99)00068-7.

Fonnesu, M., Palermo, D., Galbiati, M., Marchesini, M., Bonamini, E., Bendias, D., 2020. A new world-class deep-water play-type, deposited by the syndepositional interaction of turbidity flows and bottom currents: the giant Eocene Coral Field in northern Mozambique. Mar. Pet. Geol. 111, 179–201. https://doi.org/10.1016/j.marpetgeo.2019.07.047.

Forwick, M., Vorren, T.O., 2007. Holocene mass-transport activity and climate in outer Isfjorden, Spitsbergen: marine and subsurface evidence. The Holocene 17, 707–716. https://doi.org/10.1177/0959683607080510.

Galindo-Zaldívar, J., Balanyá, J.C., Bohoyo, F., Jabaloy, A., Maldonado, A., Martínez-Martínez, J.M., Rodríguez-Fernández, J., Suriñach, E., 2002. Active crustal fragmentation along the Scotia-Antarctic plate boundary east of the South Orkney Microcontinent (Antarctica). Earth Planet. Sci. Lett. 204, 33–46. https://doi.org/10.1016/S0012-821X(02)00959-7.

Galindo-Zaldívar, J., Puga, E., Bohoyo, F., González, F.J., Maldonado, A., Martos, Y.M., Pérez, L.F., Ruano, P., Schreider, A.A., Somoza, L., Suriñach, E., Antonio, D. De F., 2014. Magmatism, structure and age of dove Basin (Antarctica): a key to understanding South Scotia Arc development. Glob. Planet. Change 122, 50–69. https://doi.org/10.1016/j.gloplacha.2014.07.021.

García, M., Lobo, F.J., Maldonado, A., Hernández-Molina, F.J., Bohoyo, F., Pérez, L.F., 2016. High-resolution seismic stratigraphy and morphology of the Scan Basin contourite fan, southern Scotia Sea. Antarctica. Mar. Geol. 378, 361–373. https://doi.org/10.1016/j.margeo.2016.01.011.

GEBCO Compilation Group, 2020. GEBCO 2020 Grid. https://doi.org/10.5285/a29c5465-b138-234d-e053-6c86abc040b9.

Hernandez-Molina, F.J., Paterlini, M., Violante, R., Marshall, P., de Isasi, M., Somoza, L., Rebesco, M., 2009. Contourite depositional system on the argentine Slope: an exceptional record of the influence of Antarctic water masses. Geology 37, 507–510. https://doi.org/10.1130/g25578a.1.

Hernández-Molina, F.J., Soto, M., Piola, A.R., Tomasini, J., Preu, B., Thompson, P., Badalini, G., Creaser, A., Violante, R.A., Morales, E., Paterlini, M., De Santa Ana, H., 2016. A contourite depositional system along the Uruguayan continental margin: Sedimentary, oceanographic and paleoceanographic implications. Mar. Geol. 378, 333–349. https://doi.org/10.1016/j.margeo.2015.10.008.

Holder, L., Duffy, M., Opdyke, B., Leventer, A., Post, A., O'Brien, P., Armand, L.K., 2020. Controls since the mid-pleistocene transition on sedimentation and primary productivity downslope of Totten Glacier, East Antarctica. Paleoceanogr. Paleoclimatology 35. https://doi.org/10.1029/2020PA003981 e2020PA003981.

Howe, J.A., Pudsey, C.J., Cunningham, A.P., 1997. Pliocene-Holocene contourite deposition under the Antarctic Circumpolar current, western Falkland Trough, South Atlantic Ocean. Mar. Geol. 138, 27–50. https://doi.org/10.1016/S0025-3227(97)00005-4.

Jimenez-Espejo, F.J., Presti, M., Kuhn, G., McKay, R., Crosta, X., Escutia, C., Lucchi, R.G., Tolotti, R., Yoshimura, T., Ortega Huertas, M., Macrì, P., Caburlotto, A., De Santis, L., 2020. Late Pleistocene oceanographic and depositional variations along the Wilkes Land margin (East Antarctica) reconstructed with geochemical proxies in deep-sea sediments. Glob. Planet. Change 184, 103045. https://doi.org/10.1016/j.gloplacha.2019.103045.

Jullion, L., Garabato, A.C.N., Bacon, S., Meredith, M.P., Brown, P.J., Torres-Valdés, S., Speer, K.G., Holland, P.R., Dong, J., Bakker, D., Hoppema, M., Loose, B., Venables, H.J., Jenkins, W.J., Messias, M.-J., Fahrbach, E., 2014. The contribution of the Weddell Gyre to the lower limb of the Global Overturning Circulation. J. Geophys. Res. Ocean. 119, 3357–3377. https://doi.org/10.1002/2013JC009725.

King, E.L., Bøe, R., Bellec, V.K., Rise, L., Skarðhamar, J., Ferré, B., Dolan, M.F.J., 2014. Contour current driven continental slope-situated sandwaves with effects from secondary current processes on the Barents Sea margin offshore Norway. Mar. Geol. 353, 108–127. https://doi.org/10.1016/j.margeo.2014.04.003.

Knutz, P.C., Cartwright, J.A., 2004. 3D Anatomy of late Neogene Contourite Drifts and Associated Mass Flows in the Faroe-Shetland Basin. In: Davies, R.J., Cartwright, J.A., Stewart, S.A., Lappin, M., Underhill, J.R. (Eds.), 3D Seismic Technology: Application to the Exploration of Sedimentary Basins, Geological Society, London, Memoirs, 29, pp. 63–72. https://doi.org/10.1144/gsl.mem.2004.029.01.07.

Kuvaas, B., Kristoffersen, Y., Guseva, J., Leitchenkov, G., Gandjukhin, V., Løvås, O., Sand, M., Brekke, H., 2005. Interplay of turbidite and contourite deposition along the Cosmonaut Sea/Enderby Land margin, East Antarctica. Mar. Geol. 217, 143–159.

Laberg, J., Kawamura, K., Amundsen, H., Baeten, N., Forwick, M., Rydningen, T., Vorren, T., 2014. A submarine landslide complex affecting the Jan Mayen Ridge, Norwegian–Greenland Sea: slide-scar morphology and processes of sediment evacuation. Geo-Marine Lett. 34, 51–58. https://doi.org/10.1007/s00367-013-0345-z.

Larter, R.D., Hogan, K.A., Hillenbrand, C.D., Benetti, S., 2016. Debris-flow deposits on the West Antarctic continental slope. In: Dowdeswell, J.A., Canals, M., Jakobsson, M., Todd, B.J., Dowdeswell, E.K., Hogan, K.A. (Eds.), Atlas of Submarine Glacial Landforms: Modern, Quaternary and Ancient, pp. 375–376. https://doi.org/10.1144/m46.155.

Lee, J. Il, Yoon, H. Il, Yoo, K.-C., Lim, H.S., Lee, Y. Il, Kim, D., Bak, Y.-S., Itaki, T., 2012. Late Quaternary glacial–interglacial variations in sediment supply in the southern Drake Passage. Quat. Res. 78, 119–129. https://doi.org/10.1016/j.yqres.2012.03.010.

Locarnini, R.A., Whitworth III, T., Nowlin Jr., W.D., 1993. The importance of the Scotia Sea on the outflow of Weddell Sea Deep Water. J. Mar. Res. 51, 135–153. https://doi.org/10.1357/0022240933223846.

Locker, S.D., Laine, E.P., 1992. Paleogene-Neogene depositional history of the middle U. S. Atlantic continental rise: mixed turbidite and contourite depositional systems. Mar. Geol. 103, 137–164. https://doi.org/10.1016/0025-3227(92)90013-8.

Lodolo, E., Donda, F., Tassone, A., 2006. Western Scotia Sea margins: Improved constraints on the opening of the Drake Passage. J. Geophys. Res. Solid Earth 111. https://doi.org/10.1029/2006jb004361 n/a-n/a.

Lodolo, E., Civile, D., Vuan, A., Tassone, A., Geletti, R., 2010. The Scotia–Antarctica plate boundary from 35°W to 45°W. Earth Planet. Sci. Lett. 293, 200–215. https://doi.org/10.1016/j.epsl.2009.12.045.

López-Quirós, A., Lobo, F.J., Escutia, C., García, M., Hernández-Molina, F.J., Pérez, L.F., Bohoyo, F., Evangelinos, D., Salabarnada, A., Maldonado, A., Naveira Garabato, A. C., 2020. Geomorphology of Ona Basin, southwestern Scotia Sea (Antarctica): Decoding the spatial variability of bottom-current pathways. Mar. Geol. 422, 106113. https://doi.org/10.1016/j.margeo.2020.106113.

Maldonado, A., Barnolas, A., Bohoyo, F., Galindo-Zaldívar, J., Hernández-Molina, J., Lobo, F., Rodríguez-Fernández, J., Somoza, L., Tomás Vázquez, J., 2003. Contourite deposits in the central Scotia Sea: the importance of the Antarctic Circumpolar current and the Weddell Gyre flows. Palaeogeogr. Palaeoclimatol. Palaeoecol. 198, 187–221. https://doi.org/10.1016/S0031-0182(03)00401-2.

Maldonado, A., Barnolas, A., Bohoyo, F., Escutia, C., Galindo-Zaldívar, J., Hernández-Molina, J., Jabaloy, A., Lobo, F.J., Nelson, C.H., Rodríguez-Fernández, J., Somoza, L., Vázquez, J.-T., 2005. Miocene to recent contourite drifts development in the northern Weddell Sea (Antarctica). Glob. Planet. Change 45, 99–129. https://doi.org/10.1016/j.gloplacha.2004.09.013.

Maldonado, A., Bohoyo, F., Galindo-Zaldívar, J., Hernández-Molina, J., Jabaloy, A., Lobo, F., Rodríguez-Fernández, J., Suriñach, E., Vázquez, J., 2006. Ocean basins near the Scotia–Antarctic plate boundary: Influence of tectonics and paleoceanography on the Cenozoic deposits. Mar. Geophys. Res. 27, 83–107. https://doi.org/10.1007/s11001-006-9003-4.

Maldonado, A., Bohoyo, F., Galindo-Zaldívar, J., Hernández-Molina, F.J., Lobo, F.J., Lodolo, E., Martos, Y.M., Pérez, L.F., Schreider, A.A., Somoza, L., 2014. A model of oceanic development by ridge jumping: opening of the Scotia Sea. Glob. Planet. Change 123, 152–173. https://doi.org/10.1016/j.gloplacha.2014.06.010.

Martorelli, E., Bosman, A., Casalbore, D., Falcini, F., 2016. Interaction of down-slope and along-slope processes off Capo Vaticano (southern Tyrrhenian Sea, Italy), with particular reference to contourite-related landslides. Mar. Geol. 378, 43–55. https://doi.org/10.1016/j.margeo.2016.01.005.

Martos, Y.M., Maldonado, A., Lobo, F.J., Hernández-Molina, F.J., Pérez, L.F., 2013. Tectonics and palaeoceanographic evolution recorded by contourite features in southern Drake Passage (Antarctica). Mar. Geol. 343, 76–91. https://doi.org/10.1016/j.margeo.2013.06.015.

Masson, D.G., Wynn, R.B., Talling, P.J., 2010. Large landslides on passive continental margins: processes, hypotheses and outstanding questions. In: Mosher, D.C., Moscardelli, L., Baxter, C.D.P., Urgeles, R., Shipp, R.C., Chaytor, J.D., Lee, H.J. (Eds.), Submarine Mass Movements and Their Consequences. Springer Netherlands, pp. 153–165. https://doi.org/10.1007/978-90-481-3071-9_13.

McGinnis, J.P., Hayes, D.E., 1995. The roles of downslope and along-slope depositional processes: southern Antarctic Peninsula continental rise. In: Geology and Seismic Stratigraphy of the Antarctic Margin. Antarctic Research Series, 68, pp. 141–156.

McGinnis, J.P., Hayes, D.E., Driscoll, N.W., 1997. Sedimentary processes across the continental rise of the southern Antarctic Peninsula. Mar. Geol. 141, 91–109. https://doi.org/10.1016/S0025-3227(97)00056-X.

Michels, K.H., Rogenhagen, J., Kuhn, G., 2001. Recognition of contour-current influence in mixed contourite-turbidite sequences of the western Weddell Sea, Antarctica. Mar. Geophys. Res. 22, 465–485. https://doi.org/10.1023/A:1016303817273.

Michels, K.H., Kuhn, G., Hillenbrand, C.-D., Diekmann, B., Fütterer, D.K., Grobe, H., Uenzelmann-Neben, G., 2002. The southern Weddell Sea: Combined contourite-turbidite sedimentation at the southeastern margin of the Weddell Gyre. In: Stow, D. A.V., Pudsey, C.J., Howe, J.A., Faugères, J.-C., Viana, A.R. (Eds.), Deep-Water Contourite Systems: Modern Drifts and Ancient Series, Seismic and Sedimentary Characteristics, pp. 305–323. https://doi.org/10.1144/gsl.mem.2002.022.01.22.

Morozov, E.G., Demidov, A.N., Tarakanov, R.Y., Zenk, W., 2010. Source regions, abyssal pathways, and bottom flow channels (for waters of the Antarctic origin). In: Abyssal Channels in the Atlantic Ocean. Water Structure and Flows, pp. 51–98. https://doi.org/10.1007/978-90-481-9358-5_3.

Mosher, D.C., Campbell, D.C., Gardner, J.V., Piper, D.J.W., Chaytor, J.D., Rebesco, M., 2017. The role of deep-water sedimentary processes in shaping a continental margin: the Northwest Atlantic. Mar. Geol. 393, 245–259. https://doi.org/10.1016/j.margeo.2017.08.018.

Mulder, T., Faugères, J.C., Gonthier, E., 2008. Mixed turbidite–contourite systems. In: Rebesco, M., Camerlenghi, A. (Eds.), Contourites. Elsevier, Amsterdam, pp. 435–456. https://doi.org/10.1016/S0070-4571(08)10021-8.

Naveira Garabato, A.C., Heywood, K.J., Stevens, D.P., 2002a. Modification and pathways of southern ocean deep waters in the Scotia Sea. Deep. Res. Part I Oceanogr. Res. Pap. 49, 681–705. https://doi.org/10.1016/S0967-0637(01)00071-1.

Naveira Garabato, A.C., McDonagh, E.L., Stevens, D.P., Heywood, K.J., Sanders, R.J., 2002b. On the export of Antarctic bottom water from the Weddell Sea. Deep. Res. Part II Top. Stud. Oceanogr. 49, 4715–4742. https://doi.org/10.1016/S0967-0645(02)00156-X.

Nielsen, T., Kuijpers, A., 2018. Glacially influenced morphodynamic features – examples from the north Faroe margin. Mar. Geol. 402, 131–138. https://doi.org/10.1016/j.margeo.2018.01.007.

NOAA National Geophysical Data Center, 2009. ETOPO1 1 Arc-Minute Global Relief Model. NOAA National Centers for Environmental Information. https://doi.org/10.7289/V5C8276M.

Ocean Data View, 2020. https://odv.awi.de/.

Orsi, A.H., Whitworth Iii, T., Nowlin Jr., W.D., 1995. On the meridional extent and fronts of the Antarctic Circumpolar current. Deep. Res. Part I Oceanogr. Res. Pap. 42, 641–673. https://doi.org/10.1016/0967-0637(95)00021-W.

Owen, M.J., Day, S.J., Leat, P.T., Tate, A.J., Martin, T.J., 2014. Control of sedimentation by active tectonics, glaciation and contourite-depositing currents in Endurance Basin, South Georgia. Glob. Planet. Change 123, 323–343. https://doi.org/10.1016/j.gloplacha.2014.08.003.

Pérez, L.F., Hernández-Molina, F.J., Esteban, F.D., Tassone, A., Piola, A.R., Maldonado, A., Preu, B., Violante, R.A., Lodolo, E., 2015. Erosional and depositional contourite features at the transition between the western Scotia Sea and southern South Atlantic Ocean: links with regional water-mass circulation since the Middle Miocene. Geo-Marine Lett. 35, 271–288. https://doi.org/10.1007/s00367-015-0406-6.

Pérez, L.F., Bohoyo, F., Hernández-Molina, F.J., Casas, D., Galindo-Zaldívar, J., Ruano, P., Maldonado, A., 2016. Tectonic activity evolution of the Scotia-Antarctic Plate boundary from mass transport deposit analysis. J. Geophys. Res. Solid Earth 121, 2216–2234. https://doi.org/10.1002/2015JB012622.

Pérez, L.F., Maldonado, A., Hernández-Molina, F.J., Lodolo, E., Bohoyo, F., Galindo-Zaldívar, J., 2017. Tectonic and oceanographic control of sedimentary patterns in a small oceanic basin: dove basin (Scotia Sea, Antarctica). Basin Res. 29, 255–276. https://doi.org/10.1111/bre.12148.

Pérez, L.F., Martos, Y.M., García, M., Weber, M.E., Raymo, M.E., Williams, T., Bohoyo, F., Armbrecht, L., Bailey, I., Brachfeld, S., Glüder, A., Guitard, M., Gutjahr, M., Hemming, S., Hernández-Almeida, I., Hoem, F.S., Kato, Y., O'Connell, S., Peck, V.L., Reilly, B., Ronge, T.A., Tauxe, L., Warnock, J., Zheng, X., 2021. Miocene to present oceanographic variability in the Scotia Sea and Antarctic ice sheets dynamics: Insight from revised seismic-stratigraphy following IODP Expedition 382. Earth Planet. Sci. Lett. 553, 116657. https://doi.org/10.1016/j.epsl.2020.116657.

Preu, B., Hernández-Molina, F.J., Violante, R., Piola, A.R., Paterlini, C.M., Schwenk, T., Voigt, I., Krastel, S., Spiess, V., 2013. Morphosedimentary and hydrographic features of the northern argentine margin: the interplay between erosive, depositional and gravitational processes and its conceptual implications. Deep. Res. Part I Oceanogr. Res. Pap. 75, 157–174. https://doi.org/10.1016/j.dsr.2012.12.013.

Rebesco, M., 2005. Contourites. Encycl. Geol. 4, 513–527.

Rebesco, M., Pudsey, C.J., Canals, M., Camerlenghi, A., Barker, P.F., Estrada, F., Giorgetti, A., 2002. Sediment drifts and deep-sea channel systems, Antarctic Peninsula Pacific margin. In: Stow, D.A.V., Pudsey, C.J., Howe, J.A., Faugères, J.-C., Viana, A.R. (Eds.), Deep-Water Contourite Systems: Modern Drifts and Ancient Series, Seismic and Sedimentary Characteristics, pp. 353–371. https://doi.org/10.1144/gsl.mem.2002.022.01.25.

Rebesco, M., Camerlenghi, A., Van Loon, A.J., 2008. Contourite research: A field in full development. In: Rebesco, M., Camerlenghi, A. (Eds.), Contourites. Elsevier, pp. 3–10. https://doi.org/10.1016/S0070-4571(08)00201-X.

Rebesco, M., Hernández-Molina, F.J., Van Rooij, D., Wåhlin, A., 2014. Contourites and associated sediments controlled by deep-water circulation processes: State-of-the-art and future considerations. Mar. Geol. 352, 111–154. https://doi.org/10.1016/j.margeo.2014.03.011.

Rintoul, S.R., Hughes, C.W., Olbers, D., 2001. Chapter 4.6 the antarctic circumpolar current system. In: Siedler, G., Church, J., Gould, J.B.T.-I.G. (Eds.), Ocean Circulation and climate. Academic Press, pp. 271–302. https://doi.org/10.1016/S0074-6142(01)80124-8.

Ruano, P., Bohoyo, F., Galindo-Zaldívar, J., Pérez, L.F., Hernández-Molina, F.J., Maldonado, A., García, M., Medialdea, T., 2014. Mass transport processes in the southern Scotia Sea: evidence of paleoearthquakes. Glob. Planet. Change 123, 374–391. https://doi.org/10.1016/j.gloplacha.2014.06.009.

Sansom, P., 2018. Hybrid turbidite–contourite systems of the Tanzanian margin. Pet. Geosci. 24, 258–276. https://doi.org/10.1144/petgeo2018-044.

Schreider, Al A., Schreider, A.A., Galindo-Zaldivar, J., Maldonado, A., Sazhneva, A.E., Evsenko, E.I., 2018. Age of the Floors of the Protector and dove Basins (Scotia Sea). Oceanology 58, 447–458. https://doi.org/10.1134/s0001437018030177.

Solli, K., Kuvaas, B., Kristoffersen, Y., Leitchenkov, G., Guseva, J., Gandjukhin, V., 2008. The Cosmonaut Sea Wedge. Mar. Geophys. Res. 29, 51–69. https://doi.org/10.1007/s11001-008-9045-x.

Somoza, L., Medialdea, T., González, F.J., 2019. Giant mass-transport deposits in the southern Scotia Sea (Antarctica). In: Lintern, D.G., Mosher, D.C., Moscardelli, L.G., Bobrowsky, P.T., Campbell, C., Chaytor, J., Turmel, D. (Eds.), Geological Society, London. Special Publications. Geological Society, London, pp. 195–205. https://doi.org/10.1144/sp477.2.

Stow, D.A.V., Faugères, J.-C., 2008. Contourite facies and the facies model. In: Rebesco, M., Camerlenghi, A. (Eds.), Contourites. Elsevier, Amsterdam, pp. 223–256. https://doi.org/10.1016/S0070-4571(08)00213-6.

Tarakanov, R.Y., 2009. Antarctic bottom water in the Scotia Sea and the Drake Passage. Oceanology 49, 607. https://doi.org/10.1134/s0001437009050026.

Tarakanov, R.Y., 2010. Circumpolar bottom water in the Scotia Sea and the Drake Passage. Oceanology 50, 1–17. https://doi.org/10.1134/s0001437010010017.

Tucholke, B.E., Mountain, G.S., 1986. Tertiary paleoceanography of the western North Atlantic Ocean. In: Vogt, P.R., Tucholke, B.E. (Eds.), The Geology of North America, The Western North Atlantic Region, vol. M. Geological Society of America, Boulder (CO), pp. 631–650.

Uenzelmann-Neben, G., 2006. Depositional patterns at Drift 7, Antarctic Peninsula: Along-slope versus down-slope sediment transport as indicators for oceanic currents and climatic conditions. Mar. Geol. 233, 49–62. https://doi.org/10.1016/j.margeo.2006.08.008.

USGS, 2021. Earthquake Hazards Program, National Earthquake Information Center (NEIC). accessed May 28, 2021 at. https://www.earthquake.usgs.gov/earthquakes/search/.

Yin, S., Hernández-Molina, F.J., Zhang, W., Li, J., Wang, L., Ding, Weifeng, Ding, Weiwei, 2019. The influence of oceanographic processes on contourite features: a multidisciplinary study of the northern South China Sea. Mar. Geol. 415 https://doi.org/10.1016/j.margeo.2019.105967.